Sustainable Cities and Society 88 (2023) 104289

Contents lists available at ScienceDirect

Sustainable Cities and Society

journal homepage: www.elsevier.com/locate/scs

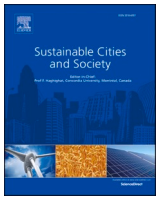

Multi-objective framework for a home energy management system with the integration of solar energy and an electric vehicle using an augmented ε-constraint method and lexicographic optimization

Truong Hoang Bao Huy [a], Huy Truong Dinh [b], Daehee Kim [a,*]

[a] Department of Future Convergence Technology, Soonchunhyang University, Asan-si, Chuncheongnam-do 31538, South Korea
[b] School of Computer Science & Engineering, The Saigon International University (SIU), Ho Chi Minh City, Viet Nam

ARTICLE INFO

Keywords:
Home energy management system (HEMS)
Multi-objective optimization
Augmented ε-constraint
Lexicographic optimization
Electric vehicle

ABSTRACT

Recent innovations in smart grid technology have increased the utilization of advanced techniques and control methods, enabling consumers to purchase and sell electricity more flexibly. Accordingly, the development of a home energy management system (HEMS) is urgently required to support residential consumers in consuming energy efficiently, achieving high satisfaction levels, and meeting grid specifications. Previous studies have only suggested simple HEMS models with one or two optimized objectives. Therefore, we propose a multi-objective mixed-integer linear programming paradigm for a comprehensive HEMS model which fully utilizes the vehicle-to-home and home-to-grid capabilities, while optimizing the energy cost, peak-to-average ratio (PAR), and discomfort index (DI). Also, an integration method of the augmented ε-constraint with lexicographic optimization is presented for effectively addressing any multi-objective HEMS problems. The proposed approach is validated across different simulations using both deterministic and stochastic models. The simulation results reveal that the energy costs and PAR can be reduced by 47.96% and 55.24%, respectively, whereas the DI is maintained at a minimum value. Extensive simulations related to the storage capacity, solar photovoltaic sizing, and uncertainty parameters are also analyzed. The proposed HEMS framework is confirmed to be a viable approach for optimally coordinating different home devices.

1. Introduction

1.1. Background

Currently, power grids are being developed using smart grid technologies and are integrated with communication and information infrastructure, offering enormous possibilities for automation and control (Batchu & Pindoriya, 2015). In the smart grid framework, the role of end users with respect to power grids has changed to that of an active market player, rather than just a passive consumer (Shafie-Khah & Siano, 2018). Accordingly, end users are more actively involved in energy trading processes. To this end, a home energy management system (HEMS) can be considered a cost-effective tool for intelligently controlling the load demand of end users at the residential level. Based on relevant input information (such as forecasted weather data, electricity price data, and limits for peak power), an HEMS is installed in a smart home to regulate the energy consumption patterns of residential users in accordance to various demand response (DR) strategies. In general, HEMSs can provide an efficient energy consumption pattern and high satisfaction to residential consumers and simultaneously support electric utilities to mitigate the peak-to-average ratio (PAR). Load patterns in the residential sector are predicted to shift even more significantly with the increasing penetration of renewable energy sources (RESs), such as solar photovoltaic (PV) systems, plug-in hybrid electric vehicles (PEVs), battery energy storage systems (BESS), heating ventilation and air conditioning (HVAC) systems, and other intelligent appliances (Batchu & Pindoriya, 2015). Therefore, an efficient HEMS structure is essential for integrating the advantages of all such electrical devices to satisfy consumer needs and preferences (Paterakis et al., 2015).

1.2. Literature review

Given the crucial role of HEMS in future smart grid development, it has attracted considerable attention, with an increasing number of related research studies in recent years (Tostado-Véliz et al., 2022a).

* Corresponding author.
E-mail addresses: trhbhuy@sch.ac.kr (T.H.B. Huy), truongdinhhuy@siu.edu.vn (H.T. Dinh), daeheekim@sch.ac.kr (D. Kim).

https://doi.org/10.1016/j.scs.2022.104289
Received 12 July 2022; Received in revised form 4 November 2022; Accepted 4 November 2022
Available online 6 November 2022

Nomenclature

Abbreviations

AUGMECON-LO	augmented ε-constraint with lexicographic optimization
BESS	battery energy storage system
EWH	electric water heater
G2H	grid-to-home
H2G	home-to-grid
H2V	home-to-vehicle
HEMS	home energy management system
HVAC	heating-ventilation-air conditioner
MILP	mixed-integer linear programming
MOEA	multi-objective evolutionary algorithm
MOP	multi-objective optimization problem
MOPSO	multi-objective particle swarm optimization
MOSGA	multi-objective search group algorithm
NSGA-II	non-dominated sorting genetic algorithm II
PDF	probability distribution function
PEV	plug-in electric vehicle
PV	photovoltaic
RES	renewable energy source
SOC	state of charge
SOE	state of energy
V2G	vehicle-to-grid
V2H	vehicle-to-home

Parameters and Variables

C_p	thermal capacity of air (kJ/kg·°C)
$C^{w,h}$	thermal capacity of hot water (kWh/°C)
COP	coefficient of performance
DI	discomfort index
DOD^{BESS}	BESS depth of discharge
DOD^{PEV}	PEV depth of discharge
K	number of controllable appliances
M	mass of air (kg)
on^k	binary variable – 1 if k^{th} controllable appliance starts the operation; otherwise 0
off^k	binary variable – 1 if k^{th} controllable appliance finishes the operation; otherwise 0
PAR	peak-to-average ratio
$P^{BESS,ch}$	BESS charging power (kW)
$\overline{P}^{BESS,ch}$	BESS charging rate (kW)
$P^{BESS,dch}$	BESS discharging power (kW)
$\overline{P}^{BESS,dch}$	BESS discharging rate (kW)
P^{CA}	power consumption of all controllable appliances (kW)
P^{EWH}	EWH power consumption (kW)
$\overline{P}^{EWH}$	EWH maximum power consumption (kW)
P^{G2H}	power purchased from the grid (kW)
$\overline{P}^{G2H}$	maximum power purchased from the grid (kW)
P^{H2G}	power sold back to the grid (kW)
$\overline{P}^{H2G}$	maximum power sold back to the grid (kW)
$P^{HVAC,c}$	HVAC cooling power consumption (kW)
$\overline{P}^{HVAC,c}$	HVAC maximum cooling power (kW)
$P^{HVAC,h}$	HVAC heating power consumption (kW)
$\overline{P}^{HVAC,h}$	HVAC maximum heating power (kW)
P^{NA}	power consumption of all non-controllable appliances (kW)
P^{peak}	peak power (kW)
$P^{PEV,ch}$	PEV charging power (kW)
$\overline{P}^{PEV,ch}$	PEV charging rate (kW)
$P^{PEV,dch}$	PEV discharging power (kW)
$\overline{P}^{PEV,dch}$	PEV discharging rate (kW)
P^{PV}	solar PV power (kW)
$\overline{P}^{PV}$	solar PV peak power (kW)
R	equivalent thermal resistance of the building (J/°C)
$R^{w,h}$	EWH thermal resistance (°C/kW)
T	number of time slots
$u^{BESS,ch}$	binary variable – 1 if BESS is charging; otherwise 0
$u^{BESS,dch}$	binary variable – 1 if BESS is discharging; otherwise 0
u^{G2H}	binary variable – 1 if power is purchased from the grid; otherwise 0
u^{H2G}	binary variable – 1 if power is sold back to the grid; otherwise 0
$u^{HVAC,c}$	binary variable – 1 if HVAC is in cooling mode; otherwise 0
$u^{HVAC,h}$	binary variable – 1 if HVAC is in heating mode; otherwise 0
u^k	binary variable – 1 if k^{th} controllable appliance is operating; otherwise 0
$u^{k,best}$	binary parameter – 1 if k^{th} controllable appliance is operating for best operation interval; otherwise 0
u^{peak}	binary variable – 1 if load pattern reaches the maximum value; otherwise 0
$u^{PEV,ch}$	binary variable – 1 if PEV is charging; otherwise 0
$u^{PEV,dch}$	binary variable – 1 if PEV is discharging; otherwise 0
V^{EWH}	EWH tank volume (gallons)
$v^{w,h}$	hot water consumption (gallons)
$\Delta\tau$	time step (hours)
δ^k	operation cycle of the k^{th} appliance (hours)
ε^{BESS}	BESS state of energy (kWh)
$\overline{\varepsilon}^{BESS}$	maximum capacity of the BESS (kWh)
ε^{PEV}	PEV state of energy (kWh)
$\overline{\varepsilon}^{PEV}$	maximum capacity of the PEV (kWh)
η^{PV}	conversion efficiency of the solar PV system
η^{BESS}	BESS charge/discharge efficiency
η^{EWH}	EWH efficiency
η^{PEV}	PEV charge/discharge efficiency
θ^{amb}	ambient temperature (°C)
$\theta^{EWH,sp}$	EWH temperature set-point (°C)
$\theta^{HVAC,sp}$	HVAC temperature set-point (°C)
θ^{in}	indoor temperature (°C)
$\overline{\theta}^{in}$	maximum indoor temperature limits (°C)
$\underline{\theta}^{in}$	minimum indoor temperature limits (°C)
$\theta^{w,c}$	inlet cold water temperature (°C)
$\theta^{w,h}$	hot water temperature (°C)
$\overline{\theta}^{w,h}$	maximum hot water temperature limit (°C)
$\underline{\theta}^{w,h}$	minimum hot water temperature limit (°C)
λ^{G2H}	purchasing electricity tariff ($/kWh)
λ^{H2G}	selling electricity tariff ($/kWh)
υ	solar irradiance (kW/m^2)
Ψ^k	allowable interval window of the k^{th} appliance

Shafie-Khah & Siano (2018) considered operational costs, response fatigue, and inhabitants' satisfaction using a stochastic HEMS model, where the results showed a 42% reduction in the electricity bill. The RES, BESS, and PEV were also considered in an HEMS model (Hou et al., 2019). Smart home planning was performed using this model to ensure the lowest bills and maximum comfort for the occupants; wherein the HEMS also optimally managed the BESS and PEV to extend their lifecycle. To minimize power consumption costs, Wang et al. (2021) proposed a refined control model using a self-adaptive discrete particle swarm algorithm for water heaters, HVAC, and PEV charging loads; RES generation and BESS were not considered in this model. Tostado-Véliz et al. (2021) suggested a solution for a smart home with an optimal capacity for BESS-PV. Their study managed demand responses and grid outages to reduce energy costs and improve system reliability. Another study focused on thermostatically controlled appliances in an off-grid smart home (Tostado-Véliz et al., 2021). The results showed that the generated power of the backup generator was decreased by 15%, whereas emissions and fuel costs were reduced by 12%. Zheng et al. (2021) used four layers in a pyramid taxonomy to design and operate a stochastic HEMS model integrated with PV-BESS. de Azevedo et al. (2022) developed a dynamic and proactive method for an HEMS considering uncertainties in prices, PV generation, and loads; this technique focused on managing PV generation and BESS. In a recent study, Tostado-Véliz et al. (2022a) proposed three demand response approaches for home-scheduling problems based on demand-flattening and peak clipping strategies. In summary, the above-cited studies mainly focused on minimizing electricity bills without considering other objectives.

The primary objective of resolving conventional HEMS optimization problems is to reduce electricity costs (Duman et al., 2021). Moreover, user preferences (i.e., waiting time and thermal comfort) should also be taken into account (Tostado-Véliz et al., 2022b). To maintain high power quality, utilities impose technical requirements on end users, such as peak load reduction and flattening of the home-load profile. Thus, the development of an HEMS for resolving multi-objective problems has attracted considerable attention. A non-dominated sorting genetic algorithm II (NSGA-II) was suggested for scheduling controllable appliances in an HEMS to reduce electricity bills and increase user comfort (Lin & Tsai, 2015). Veras et al. (2018) used NSGA-II to schedule household appliances. This model simultaneously minimized electricity costs and reduces inconvenience for residential users. A multi-objective framework was suggested for an HEMS model, which considered utility and residential objectives (Sharifi & Maghouli, 2019). To enhance the PAR and avoid high power consumption during periods of low prices, an inclining block rate tariff was combined with real-time pricing, and NSGA-II was reapplied to address the multi-objective problems. Lokeshgupta & Sivasubramani (2019) presented an HEMS model integrated with a BESS as a multi-objective mixed-integer linear programming (MILP) problem, with six case studies being conducted to analyze the effects of BESS on the proposed HEMS model. Furthermore, an economic analysis of the battery investment was also conducted. They concluded that the energy bills and peak demand were reduced to benefit both users and electric utilities. Kong et al. (2020) developed a risk-averse HEMS considering the constraints of power and risk indices to optimize the electricity cost and PAR. Lu et al. (2022) developed a coding genetic algorithm combined with niche technology for an efficient HEMS model in smart homes. This study aimed to decrease the peak load value and electricity cost, by applying the tracing Pareto approach using the weighted sum technique. Similarly, Yu et al. (2022) developed a multi-objective HEMS model which enabled smart device planning to minimize electricity bills and peak-to-valley electricity consumption. This study also examined the peak-shaving effect and its impact on grid investment and power sources. Nevertheless, the major drawback of the aforementioned studies is that the HEMS model is relatively simple with respect to shiftable devices, solar PV generation, and BESS. HEMS only acted as a passive load on the utility grid in the cited studies; hence, the energy injected energy back into the grid was not considered. Moreover, bidirectional PEVs have also not been addressed.

Recently, new HEMS models have been developed by assuming the HEMS as an active load (i.e., a prosumer). Anvari-Moghaddam et al. (2015) developed a multi-objective MILP model, which acted as an active load, to optimize energy usage and maximize thermal comfort in a smart home. Thermal comfort was increased by adjusting the underfloor heating and cooling setpoints. Rahim et al. (2016) evaluated the performance of different heuristic methods, which included genetic algorithm, binary particle swarm optimization, and ant colony optimization, to address the HEMS optimization requirements. Electricity bills and waiting times were considered, where the electricity bill was a combination of time-of-use tariffs and inclined block rates. The authors indicated that the binary particle swarm optimization obtained better results than other methods in solving HEMS problems. A user-centric HEMS called Foresee was introduced as an active prosumer to optimize various objective functions, including energy bills, user convenience, thermal comfort, and carbon emissions (Jin et al., 2017). Zupančič et al. (2020) introduced an active HEMS based on optimized decision trees. Multi-objective genetic programming was used to optimize the cost, and cost versus green objective functions. Javadi et al. (2020, 2021) proposed a multi-objective MILP problem for an HEMS incorporating a solar PV panel and a BESS. The model considered three pricing options (time-of-use, critical peak pricing, and real-time pricing) to encourage demand-side participation in the power grid. Javadi et al. (2020) combined all the objectives into a single objective function based on the weighted sum method, whereas Javadi et al. (2021) considered the daily bill as the main goal and the discomfort index as a constraint using the epsilon constraint method. Wang et al. (2021) developed a general HEMS model based on the Internet of Things. Subsequently, a modified butterfly optimization algorithm was applied to address the HEMS problem with two objectives: user satisfaction and energy cost. Emami Javanmard et al. (2020) proposed a combined model involving solar PV, solar thermal, wind turbine, and fuel cells to decrease energy consumption and emissions in a building. Similarly, Esmaeel Nezhad et al. (2021) presented a multi-objective self-scheduling problem for a household with comprehensive HVAC modeling, BESS, and PV systems. Their proposed model optimized daily electricity bills by considering time-of-use tariffs. However, these reports either did not consider the PEV or considered only the home-to-vehicle (H2V) mode of the PEV in HEMS modeling. As the PEVs can now be charged and discharged at home using advanced technologies, PEV operations can affect both the electricity generation and consumption patterns of households.

In general, HEMS models have been designed with only two objective functions, namely, energy cost and user comfort; and energy cost and PAR. Two-objective optimization models can be solved straightforwardly using the weighted sum approach or multi-objective evolutionary algorithms. Several studies have proposed HEMS models with more than two objectives. Khalid et al. (2018) applied hybrid bacterial foraging and genetic algorithm to minimize electricity costs, user comfort, and PAR through a load-shifting strategy. The authors also applied dynamic programming to address real-time scheduling as a knapsack problem. The proposed approach was evaluated using three pricing strategies: real-time pricing, time-of-use, and critical peak pricing. Yahia & Pradhan (2020) suggested a multi-objective model for optimizing the energy cost, peak load, and inconvenience level, wherein the time-of-use tariff was considered. Three methods, namely, compromise optimization, preemptive optimization, and the normalized weighted-sum method, were applied to deal with HEMS problems. The proposed solutions considerably reduced the energy cost, eliminated user discomfort, and reduced the peak home loads. Tostado-Véliz et al. (2022b) suggested multi-objective modeling for an HEMS by considering different objective functions. They used lexicographic optimization and scalarizing functions, selecting the electricity bill as the most important factor, and treated other objectives as secondary. In the aforementioned

studies, the home-to-grid (H2G) and vehicle-to-home (V2H) functions were not covered in the HEMS models. These cited works only treated the HEMS as a passive load, which was a major limitation.

1.3. Research gaps and motivation

From the perspective of the literature review, a considerable amount of research on HEMS modeling has been conducted for both single- and multi-objective problems. Table 1 presents a brief comparison of the research on HEMS optimization. As can be inferred from Table 1, the research gaps in the HEMS optimization study are as follows:

- In general, the HEMS models proposed in the literature are simplistic. The references focused only on scheduling controllable appliances, RESs, and BESS. Some appliances and functions of HEMS, such as thermostatically controlled appliances and V2H, have not been fully utilized. Furthermore, most previous studies have considered HEMS as a passive consumer instead of an active prosumer, and the possibility of selling electricity to the grid has been neglected. Only a handful of studies have proposed a comprehensive HEMS model, yet these works have only considered the single objective of electricity cost reduction. The HEMS scheduling problem can be more realistic and comprehensive when all the aforementioned factors are considered in a multi-objective paradigm.
- The HEMS optimization problem in the literature has been studied extensively with two objectives: either energy cost and PAR or energy cost and user satisfaction. Optimization problems are multi-objective in nature; therefore, an HEMS problem should cover all three aspects: economic, technical, and user satisfaction. This is intended to provide users with a solution that compromises all the objectives. Ignoring any of these objectives may cause the HEMS model to become unbalanced and unrealistic. Only a few studies have addressed the HEMS problem with more than two objectives. However, these studies defined HEMS as a passive load rather than an active load, and bidirectional PEVs were not addressed.
- Dealing with multi-objective problems raises several challenges, moreover, increasing the number of objective functions requires more computational time to determine the Pareto optimal front. In previous literature, multi-objective problems of HEMS were solved using three main approaches: mathematical optimization-based approaches, heuristic-based approaches, and multi-objective evolutionary algorithms (MOEAs). In this regard, a straightforward method is to convert a multi-objective problem into a single-objective problem using the weighted-sum method. The weighting factors of the objective functions were chosen based on the decision maker, where the more important goal was assigned a higher weight. After aggregation, the problem can be solved using mathematical optimization-based or heuristic-based approaches. Although this

Table 1
Summary of the reviewed references and the current study in terms of HEMS optimization.

Refs.	Controllable devices	Thermostatically controlled appliances	RES	BESS	Bidirectional PEV	Objective			Method	Prosumer
						Energy cost	User comfort	PAR		
Shafie-Khah & Siano (2018)	✓	✓	✓	✓	✓	✓			MILP	✓
Hou et al. (2019)	✓	✓	✓	✓	✓	✓			MILP	✓
Wang et al. (2021)	x	✓	x	x	✓	✓			Metaheuristic	✓
Tostado-Véliz et al. (2021)	✓	x	✓	✓	x	✓			MILP	✓
Tostado-Véliz et al. (2021)	x	✓	✓	✓	x	✓			MILP	x
Zheng et al. (2021)	✓	x	✓	✓	x	✓			Nonlinear	✓
de Azevedo et al. (2022)	✓	x	✓	✓	x	✓			MILP	✓
Tostado-Véliz et al. (2022a)	✓	✓	✓	✓	✓	✓			MILP	✓
Lin & Tsai (2015)	✓	x	x	x	x	✓	✓		NSGA-II	x
Veras et al. (2018)	✓	x	x	x	x	✓	✓		NSGA-II	x
Sharifi & Maghouli (2019)	✓	x	x	✓	x	✓	✓		NSGA-II	x
Lokeshgupta & Sivasubramani (2019)	✓	x	x	✓	x	✓		✓	MILP – weighted sum	x
Kong et al. (2020)	✓	✓	✓	x	x	✓		✓	genetic algorithm	x
Lu et al. (2022)	✓	x	x	x	x	✓		✓	genetic algorithm	x
Yu et al., (2022)	✓	x	x	x	x	✓		✓	NSGA-II	x
Anvari-Moghaddam et al. (2015)	✓	✓	x	✓	x	✓	✓		MINLP – weighted sum	✓
Rahim et al. (2016)	✓	x	✓	✓	x	✓	✓		heuristic algorithms – weighted sum	✓
Jin et al. (2017)	✓	✓	✓	✓	x	✓	✓		model predictive control	✓
Zupančič et al. (2020)	✓	x	✓	✓	x	✓		✓	genetic algorithm	✓
Javadi et al. (2020)	✓	x	✓	✓	x	✓	✓		MILP – weighted sum	✓
Javadi et al. (2021)	✓	x	✓	✓	x	✓	✓		MILP – epsilon-constraint	✓
Wang et al. (2021)	✓	✓	✓	✓	x	✓	✓		Heuristic algorithm – weighted sum	✓
Khalid et al. (2018)	✓	x	x	x	x	✓	✓	✓	Heuristic algorithm – weighted sum	x
Yahia & Pradhan (2020)	✓	x	x	x	x	✓	✓	✓	MILP – weighted sum	x
Tostado-Véliz et al. (2022b)	✓	✓	✓	✓	x	✓	✓	✓	MILP – lexicographic & scalarizing functions	x
Present study	✓	✓	✓	✓	✓	✓	✓	✓	MILP – AUGMECON-LO	✓

technique is straightforward and has a low computational cost, it is difficult to generate diverse solutions for the Pareto optimal front. Accordingly, the obtained solution may not be a compromise solution for all objectives. Many studies have proposed solutions based on MOEAs. As MOEAs are stochastic in nature, they can become stuck in local optimality and converge prematurely, making it difficult to reach a global optimal solution. Moreover, MOEAs require considerable computational time. Therefore, it is necessary to propose a powerful method to efficiently solve multi-objective HEMS problems within a low computation time.

- The integration of solar PV systems and PEVs is becoming increasingly common in smart homes. Nevertheless, scheduling for solar PV and PEV poses some difficulties owing to the unpredictable and intermittent nature of weather and users. Many previous studies ignored the uncertainty of these parameters and only considered day-ahead data for an HEMS model. For a comprehensive evaluation, an HEMS should be formulated using both deterministic and stochastic models.

1.4. Research contributions

Previous studies have not investigated multi-objective optimization problems (MOPs) for comprehensive HEMS modeling in the electricity market. Inspired by the above motivations and research gaps, we herein propose a comprehensive multi-objective paradigm for HEMS with the penetration of RES, BESS, and PEV under energy trading, where HEMS can act as an active prosumer. The energy cost, PAR, and discomfort index (DI) are fully considered to satisfy the important elements of the competitive HEMS model. The proposed method integrates the augmented ε-constraint method and lexicographic optimization (AUGMECON-LO) to address the multi-objective MILP problem for HEMS. To the best of our knowledge, this study is the first attempt to propose AUGMECON-LO for resolving a comprehensive multi-objective HEMS paradigm with three objectives. The proposed method is validated using a typical smart-home model with various scenarios. The ε-constraint method is one of the most efficient approaches for addressing MOPs (Aghaei et al., 2009; Amjady et al., 2009; Roman & Rosehart, 2006). The basic concept of the ε-constraint method is to consider one objective as the main objective, whereas the other objectives are treated as constraints. The AUGMECON-LO has been suggested to overcome the limitations of the original version, and to more efficiently obtain Pareto optimal solutions (Javadi et al., 2021; Nezhad et al., 2014; Roman & Rosehart, 2006). The main contributions of this study are as follows:

- A comprehensive model for an HEMS is proposed under a smart grid framework that includes controllable appliances, thermostatically controlled appliances, solar PV generation, BESS, and bidirectional PEVs. The proposed HEMS supports residential end users to actively participate in the power grid, where they can flexibly produce, sell, trade, or store energy.
- The mathematical model of the HEMS is formulated as a multi-objective MILP problem to efficiently achieve a global solution. Three different objective functions are considered for the HEMS optimization problem: economic, technical, and user convenience. Furthermore, three expansion cases, namely unavailability of the V2H capability, unavailability of BESS, and unavailability of both V2H capability and BESS, are simulated to study the impact of storage capacity on the HEMS in terms of the three objective functions under study.
- An effective AUGMECON-LO method is developed to address the multi-objective paradigm of the HEMS optimization problem. First, lexicographic optimization is used to define the payoff table. The augmented ε-constraint approach can then effectively obtain efficient Pareto optimal solutions and avoid inefficient ones. Finally, a fuzzy decision-making method is applied to select the compromise solution from the set of obtained Pareto optimal solutions. The proposed algorithm is compared with other well-regarded MOEAs. The comparison results indicate that the proposed method can achieve a superior compromise solution with a low computation time. In particular, the proposed method achieves the best compromise solution with an energy cost of 0.6841, PAR of 1.3639, and DI of 0, which is superior to the solutions achieved by other MOEAs.
- A stochastic model related to uncertainty in weather data and the state of energy of a PEV is investigated for a multi-objective HEMS optimization problem by applying a scenario-based approach. To this end, probability distribution functions are used to model the uncertain nature of solar irradiation, ambient temperature, and the initial state of energy of the PEV. Furthermore, scenario reduction based on the k-medoids technique is implemented to ensure a reasonable number of scenarios for effective computation.

1.5. Paper layout

Section 2 outlines the problem formulation for HEMS modeling. The proposed augmented ε-constraint method and lexicographic optimization are described in Section 3. The simulation results are discussed in Sections 4, and 5 provides concluding statements.

2. Problem formulation

This study aims to develop a comprehensive HEMS that integrates solar PV generation, controllable appliances, thermostatically controlled appliances, BESS, and PEV in a typical smart home. Also, V2H and H2G capacities are fully utilized. Fig. 1 depicts a typical smart home investigated for this study. A smart home includes the following main components and devices:

- Solar PV system: A small solar-powered generator is installed to generate clean and sustainable energy. The output of a solar-powered generator depends on weather factors such as solar irradiation and ambient temperature.
- Non-controllable appliances: These appliances, such as refrigerators, televisions, or lights, are used based on user preferences. Their operation schedule is fixed and cannot be managed using HEMS.
- Controllable appliances: Each controllable appliance has a specific duty cycle and power consumption. Within the allowed intervals, the operation interval of controllable appliances can be shifted during times of low electricity cost to minimize the total daily energy cost.
- Thermostatically controlled appliances: HVAC and EWH systems are considered under this type of appliance. With predefined temperature setpoints, these appliances are controlled at the optimal mode and power consumption to maintain the room and water temperatures within the allowable range.

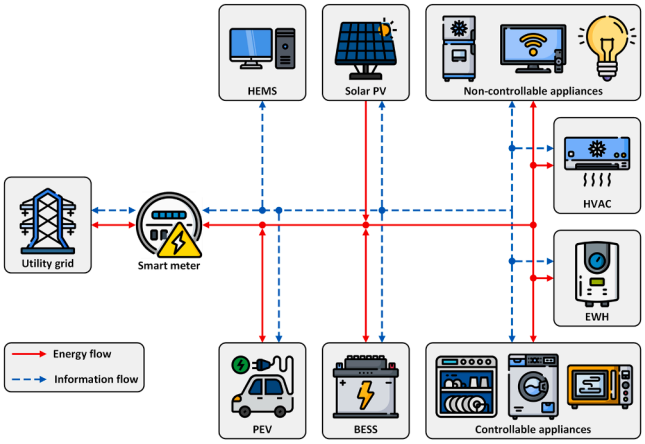

Fig. 1. Schematic of the proposed HEMS.

- BESS: It stores energy from solar arrays or the electric grid and provides energy to home-load demands. The BESS is intelligently coordinated to decide when to store energy as reserves or release energy to the home loads and grid. Energy may be released from the BESS during peak demand intervals, thereby reducing the energy cost and load patterns.
- PEV: With smart technologies, PEVs can interact with the home in more advanced ways than simply charging. Thus, the V2H capability of the PEV is fully utilized in this study. When plugged in at home, the PEV is intelligently charged at times of low cost and low demand, while providing backup power for the residential user.
- HEMS: It is used to efficiently manage energy usage and provide a stable source of power to meet the energy needs of residential users. An HEMS optimizes the operation schedule of solar PV generation, controllable appliances, thermostatically controlled appliances, BESS, and PEV in a coordinated manner with the aim of reducing energy costs, reducing PAR, and improving user convenience.

In an HEMS, the communication network is utilized to relay information between the HEMS, utility grid, and user. The HEMS receives and regulates data and communications from users, devices, and external sources. The input data transferred to the HEMS consist of the duty cycle and energy consumption of controllable appliances, state of energy of the PEV and BESS, forecasted solar irradiation, and forecasted ambient temperature. Additionally, the proposed algorithm is embedded in the HEMS to analyze the necessary information and energy consumption data, and then optimize the operation schedule of all devices. Accordingly, the HEMS sends control signals to all devices for the scheduled operation. As a smart prosumer, the proposed HEMS can purchase or sell energy flexibly with the utility grid. The smart meter is a communication device between the HEMS and utility grid. The smart meter provides an HEMS with predefined electricity tariffs from the utility grid. It also receives information from the HEMS regarding the amount of energy exchanged with the utility grid. Household loads are supplied by the utility grid, solar PV generation, and storage capacity of the BESS and PEV. Moreover, surplus energy from solar PV, BESS, and PEV can be sold back to the grid at any interval for profit.

Moreover, this study considers some assumptions for the HEMS paradigm as follows:

- The effects of battery degradation of the BESS and PEV due to charging/discharging cycles are ignored. As for the PEV, residential users may participate in the battery leasing services provided by the PEV manufacturers (Paterakis et al., 2015). Accordingly, the PEV battery is replaced for a monthly fee when its charging capacity drops below a certain level.
- For simplicity, the maintenance and degradation costs of solar PV systems and BESS are not taken into account (Paterakis et al., 2015; Shafie-Khah & Siano, 2018).
- The HEMS is assumed to receive all required forecasted data, including solar irradiation, ambient temperature, and the initial state of energy of the PEV (Tostado-Véliz et al., 2022a).

The proposed HEMS is formulated as an MILP problem over 24 h of a day with 48 intervals ($T = 48$) and a time step of 30 min ($\Delta\tau = 0.5$). The mathematical model of each component of the HEMS paradigm and the objective functions to be optimized are detailed in the following subsections.

2.1. Smart home energy management modeling

2.1.1. Grid modeling

In a prosumer environment, an HEMS can either purchase or sell energy to the utility grid. Owing to the physical limitations of the distributed grid or power purchase agreement, the amount of electricity traded between households and the grid is limited by utility companies. Grid modeling can be expressed as follows (Tostado-Véliz et al., 2021, 2022a):

$$0 \le P_t^{G2H} \le u_t^{G2H} \cdot \overline{P}^{G2H}; \forall t = 1, 2, \ldots, T \tag{1}$$

$$0 \le P_t^{H2G} \le u_t^{H2G} \cdot \overline{P}^{H2G}; \forall t = 1, 2, \ldots, T \tag{2}$$

where P_t^{G2H} is the power purchased from the grid at interval t, P_t^{H2G} is the power sold back to the grid at interval t, $\overline{P}^{G2H}$ and $\overline{P}^{H2G}$ are the maximum powers that can be purchased and sold between HEMS and the utility grid, respectively, and u_t^{G2H} and u_t^{H2G} are the binary representations of the purchase and sell modes of the HEMS with the utility grid at interval t, respectively.

The purchasing and selling processes for energy are assumed to be impossible simultaneously, which is imposed by the following constraint (Tostado-Véliz et al., 2021; Tostado-Véliz et al., 2022a):

$$0 \le u_t^{G2H} + u_t^{H2G} \le 1; \forall t = 1, 2, \ldots, T \tag{3}$$

2.1.2. PV system modeling

Generally, an HEMS can define the day-ahead expected solar PV output based on weather forecasts such as ambient temperature and solar irradiation. Accordingly, the instantaneous maximum power generated by the solar PV at time interval t is determined as follows (Tostado-Véliz et al., 2021; Tostado-Véliz et al., 2022b):

$$\phi_t^{PV} = \overline{P}^{PV} \cdot \left[0.25 \cdot \upsilon_t + 0.03 \cdot \upsilon_t \cdot \theta_t^{amb} + \left(1.01 - 1.13 \cdot \eta^{PV}\right) \cdot \upsilon_t^2\right]; \forall t = 1, 2, \ldots, T \tag{4}$$

where υ_t is the solar irradiance at interval t, $\overline{P}^{PV}$ is the solar PV peak power, θ_t^{amb} is the ambient temperature at interval t, and η^{PV} is the conversion efficiency.

The output of the solar PV system, as shown in Eq. (4) may yield a value higher than the peak power. Therefore, a constraint (Eq. (5)) is imposed to limit the expected power output of the solar PV so as not to exceed the peak power (Tostado-Véliz et al., 2022a):

$$0 \le P_t^{PV} \le \begin{cases} \phi_t^{PV} & \text{if} \phi_t^{PV} \le \overline{P}^{PV} \\ \overline{P}^{PV} & \text{otherwise} \end{cases}; \quad \forall t = 1, 2, \ldots, T \tag{5}$$

2.1.3. Controllable appliance modeling

In a typical smart home, the appliances operate in a predetermined cycle. HEMS can switch operations to utilize periods of low electricity prices. The controllable appliances are modeled using Eqs. (6)–(9). Equality constraint (Eq. (6)) ensures that controllable appliances must complete their operation cycle in the allowable interval window (Tostado-Véliz et al., 2022b):

$$\sum_{t=1}^{T} \left\{u_t^k\right\} = \delta^k; \forall t \in \Psi^k, k = 1, 2, \ldots, K \tag{6}$$

where u_t^k denotes the binary variable of commitment status for the k^{th} appliance at time interval t, δ^k is the operation cycle of the k^{th} appliance, and Ψ^k is the allowable interval window of the k^{th} appliance. From Eq. (6), the total number of intervals for which a controllable appliance is operated within its allowable interval window (Ψ) is equal to the corresponding predefined operation cycle (δ).

In this study, the operations of controllable appliances are assumed to be uninterrupted once activated. Controllable appliances must be continuously operated and cannot be interrupted until their operation cycles are completed, which can be imposed, as in Eq. (7) (Paterakis et al., 2015):

$$u_t^k - u_{t-1}^k = on_t^k - off_t^k; \forall t = 1, 2, \ldots, T, k = 1, 2, \ldots, K \tag{7}$$

where on_t^k/off_t^k is equal to one if the k^{th} appliance starts/ finishes operation at interval t; otherwise, on_t^k/off_t^k is equal to zero.

Moreover, it is assumed that controllable appliances can only be activated once during the scheduling period, as stated in Eq. (8) as follows (Tostado-Véliz et al., 2022b):

$$\sum_{t=1}^{T}\{on_t^k\}=1;\forall k=1,2,\ldots,K \tag{8}$$

The power consumption of all controllable appliances at each interval is defined by Eq. (9):

$$P_t^{CA}=\sum_{k=1}^{K}\left(u_t^k\cdot P^k\right) \tag{9}$$

where P_t^{CA} is the power consumption of all controllable appliances at interval t and P^k is the hourly power consumption of the k^{th} appliance.

2.1.4. BESS modeling

Modern smart homes are typically equipped with a BESS for economic and technical benefits. Depending on the mode of operation (charging or discharging), the BESS can operate both an energy consumer and a power source. When the BESS is in the charging mode as a load, the HEMS adjusts the BESS to stop discharging on schedule and shifts its discharging state to another interval. As shown in Eq. (10), the state of energy (SOE) of the BESS at interval t is a function of the SOE at interval $(t-1)$, energy charged to the BESS, and energy discharged back to the HEMS and grid at interval t. The amount of energy stored in the BESS is bounded by its depth of discharge (DOD) and maximum capacity, as expressed in Eq. (11). Hence, the BESS is modeled as follows (Alsaidan et al., 2018; Arévalo et al., 2021):

$$\varepsilon_t^{BESS}=\varepsilon_{t-1}^{BESS}+\left(\eta^{BESS}\cdot P_t^{BESS,ch}-\frac{P_t^{BESS,dch}}{\eta^{BESS}}\right)\cdot\Delta\tau;\forall t=1,2,\ldots,T \tag{10}$$

$$\left(1-DOD^{BESS}\right)\cdot\overline{\varepsilon}^{BESS}\le\varepsilon_t^{BESS}\le\overline{\varepsilon}^{BESS};\forall t=1,2,\ldots,T \tag{11}$$

where ε_t^{BESS} is the SOE of the BESS at interval t; $P_t^{BESS,ch}$ and $P_t^{BESS,dch}$ are the BESS charging and discharging powers at interval t, respectively; η^{BESS} is the charge/discharge efficiency of the BESS; $\overline{\varepsilon}^{BESS}$ is the maximum capacity of the BESS; and DOD^{BESS} is the DOD of the BESS.

In Eqs. (12) and (13), the charging and discharging powers are restricted to the rated power. Inequality (14) also prevents the BESS charging and discharging modes from occurring simultaneously (Tostado-Véliz et al., 2022a, 2022b).

$$0\le P_t^{BESS,ch}\le u_t^{BESS,ch}\cdot\overline{P}^{BESS,ch};\forall t=1,2,\ldots,T \tag{12}$$

$$0\le P_t^{BESS,dch}\le u_t^{BESS,dch}\cdot\overline{P}^{BESS,dch};\forall t=1,2,\ldots,T \tag{13}$$

$$0<u_t^{BESS,ch}+u_t^{BESS,dch}\le 1;\forall t=1,2,\cdots,T \tag{14}$$

where $u_t^{BESS,ch}$ and $u_t^{BESS,dch}$ are the binary representations of the BESS charge and discharge modes at interval t, respectively; $\overline{P}^{BESS,ch}$ and $\overline{P}^{BESS,dch}$ are the BESS charging and discharging rates, respectively.

This study assumes that the energy stored in the BESS is set to the maximum capacity at the initial and final intervals of the scheduling period based on Eq. (15) (Tostado-Véliz et al., 2022b):

$$\varepsilon_1^{BESS}=\varepsilon_T^{BESS}=\overline{\varepsilon}^{BESS} \tag{15}$$

2.1.5. PEV modeling

The PEV modeling is similar to the BESS model described in the previous subsection. However, the PEV is not available at home during specific intervals, and is only involved in the scheduling horizon once it returns home. In addition to charging batteries, PEVs supply energy to households or even sell energy to the utility grid to fully utilize their capabilities. Eq. (16) models the SOE of the PEV at interval t as a function of the SOE at interval $(t-1)$, energy charged to the PEV, and energy discharged to the HEMS and utility grid at interval t. The energy stored in the PEV battery must be restricted to the DOD and must not be overcharged using constraint (17). Therefore, the PEV model can be mathematically defined as follows (Alsaidan et al., 2018; Tostado-Véliz et al., 2021):

$$\varepsilon_t^{PEV}=\varepsilon_{t-1}^{PEV}+\left(\eta^{PEV}\cdot P_t^{PEV,ch}-\frac{P_t^{PEV,dch}}{\eta^{PEV}}\right)\cdot\Delta\tau;\forall t=1,2,\ldots,T \tag{16}$$

$$(1-DOD)\cdot\overline{\varepsilon}^{PEV}\le\varepsilon_t^{PEV}\le\overline{\varepsilon}^{PEV};\forall t=1,2,\ldots,T \tag{17}$$

where ε_t^{PEV} is the SOE of the PEV at time interval t; $P_t^{PEV,ch}$ and $P_t^{PEV,dch}$ are the PEV charging and discharging powers at time interval t, respectively; η^{PEV} is the charge/discharge efficiency of the PEV; $\overline{\varepsilon}^{PEV}$ is the maximum capacity of the PEV; and DOD^{PEV} is the DOD of the PEV.

Eqs. (18) and (19) limit the charge and discharge power of the PEV. Moreover, the PEV cannot charge and discharge simultaneously according to Eq. (20) (Tostado-Véliz et al., 2022a).

$$0\le P_t^{PEV,ch}\le u_t^{PEV,ch}\cdot\overline{P}^{PEV,ch};\forall t=1,2,\ldots,T \tag{18}$$

$$0\le P_t^{PEV,dch}\le u_t^{PEV,dch}\cdot\overline{P}^{PEV,dch};\forall t=1,2,\ldots,T \tag{19}$$

$$0<u_t^{PEV,ch}+u_t^{PEV,dch}\le 1;\forall t=1,2,\ldots,T \tag{20}$$

where $u_t^{PEV,ch}$ and $u_t^{PEV,dch}$ are the binary representations of the PEV charge and discharge state modes at time interval t, respectively; $\overline{P}^{PEV,ch}$ and $\overline{P}^{PEV,dch}$ are the PEV charging and discharging rates, respectively.

Eq. (21) indicates that the initial SOE of the PEV battery is equal to the remaining energy when the PEV arrives at home. The PEV should be fully charged at departure time, which is defined in Eq. (22) (Tostado-Véliz et al., 2022a, 2022b).

$$\varepsilon_{arrive}^{PEV}=\varepsilon_{initial}^{PEV} \tag{21}$$

$$\varepsilon_{depart}^{PEV}=\overline{\varepsilon}^{PEV} \tag{22}$$

2.1.6. HVAC modeling

To maintain the room temperature within acceptable limits, we consider the HVAC system as a thermostatically controlled appliance in both heating and cooling modes. Based on a linearized model of the thermal inertia of buildings, the indoor temperature is a function of HVAC power consumption and outdoor temperature, as follows (Paterakis et al., 2015; Wang et al., 2013):

$$\theta_t^{in}=\left(1-\frac{\Delta\tau}{10^3\cdot M\cdot C_p\cdot R}\right)\cdot\theta_{t-1}^{in}+\frac{\Delta\tau}{10^3\cdot M\cdot C_p\cdot R}\cdot\theta_{t-1}^{amb}+\frac{\Delta\tau\cdot\left(P_{t-1}^{HVAC,h}-P_{t-1}^{HVAC,c}\right)}{0.000277\cdot M\cdot C_p}\cdot COP;\ \forall t=1,2,\ldots,T \tag{23}$$

where θ_t^{in} is the indoor temperature at interval t; R is the equivalent thermal resistance of the building; C_p and M are the thermal capacity and mass of air, respectively; $P_t^{HVAC,h}$ and $P_t^{HVAC,c}$ are the heating and cooling power consumption of the HVAC at interval t, respectively; and COP is the coefficient of performance of the HVAC.

The HVAC power consumption for heating and cooling is limited by its rated power according to Eqs. (24) and (25), respectively. Moreover, the heating and cooling modes of the HVAC system may operate only at different time intervals, which can be limited to Eq. (26) (Tostado-Véliz et al., 2021).

$$0\le P_t^{HVAC,h}\le u_t^{HVAC,h}\cdot\overline{P}^{HVAC,h};\quad\forall t=1,2,\ldots,T \tag{24}$$

$$0 \le P_t^{HVAC,c} \le u_t^{HVAC,c} \cdot \overline{P}^{HVAC,c}; \quad \forall t = 1,2,\ldots,T \tag{25}$$

$$0 \le u_t^{HVAC,h} + u_t^{HVAC,c} \le 1; \quad \forall t = 1,2,\ldots,T \tag{26}$$

where $\overline{P}^{HVAC,h}$ and $\overline{P}^{HVAC,c}$ are the maximum heating and cooling powers, respectively, and $u_t^{HVAC,h}$ and $u_t^{HVAC,c}$ are the binary representations of the heating and cooling modes, respectively, at time interval t.

With HVAC operation, the indoor temperature must be maintained within acceptable limits as follows (Tostado-Véliz et al., 2021):

$$\underline{\theta}^{in} \le \theta_t^{in} \le \overline{\theta}^{in}; \forall t = 1,2,\ldots,T \tag{27}$$

where $\overline{\theta}^{in}$ and $\underline{\theta}^{in}$ denote the maximum and minimum indoor temperature limits, respectively.

We assume that the temperatures at the initial and final intervals are fixed to the set point ($\theta^{HVAC,sp}$), as in constraint (28) (Tostado-Véliz et al., 2021).

$$\theta_1^{in} = \theta_T^{in} = \theta^{HVAC,sp} \tag{28}$$

2.1.7. EWH modeling

A linearized model is used to model the EWH as a function of the hot water temperature at the previous interval and the heat transfer effect on the environment and EWH operation, as expressed in Eq. (29) (Du & Lu, 2011; Paterakis et al., 2015):

$$\theta_{t+1}^{w,h} = \theta_t^{w,h} + \Delta\tau \cdot P_t^{EWH} \cdot \eta^{EWH} \cdot C^{w,h} - \left(\theta_t^{in} - \theta_t^{w,h}\right) e^{\left(\frac{-\Delta\tau}{R^{w,h} \cdot C^{w,h}}\right)}; \forall t = 1,2,\ldots,T, v_t^{w,h} = 0 \tag{29}$$

where $\theta_t^{w,h}$ is the hot water temperature at interval t, P_t^{EWH} is the EWH power consumption at interval t, η^{EWH} is the EWH efficiency, $C^{w,h}$ is the thermal capacity of water, $R^{w,h}$ is the thermal resistance of EWH, and $v_t^{w,h}$ is the hot water consumption at interval t.

As hot water is drawn from the EWH system for consumption at certain intervals, the inlet cold water is replenished to the EWH system, and the hot water temperature can be defined as follows (Paterakis et al., 2015; Tostado-Véliz et al., 2021):

$$\theta_{t+1}^{w,h} = \frac{\theta_t^{w,h} \cdot \left(V^{EWH} - v_t^{w,h}\right) + \theta^{w,c} \cdot v_t^{w,h}}{V^{EWH}}; \forall t = 1,2,\ldots,T, v_t^{w,h} > 0 \tag{30}$$

where $\theta^{w,c}$ is the inlet cold water temperature and V^{EWH} is the EWH tank volume.

Constraint (31) sets limitations on the power consumption of the EWH. Conversely, a specified bound is also imposed for the hot-water temperature, as in Eq. (32) (Tostado-Véliz et al., 2021).

$$0 \le P_t^{EWH} \le \overline{P}^{EWH}; \quad \forall t = 1,2,\ldots,T \tag{31}$$

$$\underline{\theta}^{w,h} \le \theta_t^{w,h} \le \overline{\theta}^{w,h}; \forall t = 1,2,\ldots,T \tag{32}$$

where $\overline{P}^{EWH}$ is the maximum power consumption of the EWH; and $\overline{\theta}^{w,h}$ and $\underline{\theta}^{w,h}$ denote the maximum and minimum hot water temperature limits, respectively.

At the initial and final intervals, it is assumed that the hot water temperatures are equal to the set point ($\theta^{EWH,sp}$), as follows (Tostado-Véliz et al., 2021):

$$\theta_1^{w,h} = \theta_T^{w,h} = \theta^{EWH,sp} \tag{33}$$

2.1.8. Home energy balance

The proposed HEMS model ensures that all loads are served, and the home energy balance is given as follows (Shafie-Khah & Siano, 2018):

$$P_t^{G2H} + P_t^{PV} + P_t^{BESS,dch} + P_t^{PEV,dch} = P_t^{H2G} + P_t^{NA} + P_t^{CA} + P_t^{BESS,ch} + P_t^{PEV,ch} + P_t^{HVAC,h} + P_t^{HVAC,c} + P_t^{EWH}; \quad \forall t = 1,2,\ldots,T \tag{34}$$

where P_t^{NA} is the power consumption of all non-controllable appliances at interval t.

2.2. Objective function

The main goal of the HEMS model is to determine the best values for the decision variables to optimize a set of predefined objective functions while satisfying inequality and equality constraints. Mathematically, the multi-objective optimization of the HEMS problem can be expressed as follows:

$$\min f(\boldsymbol{x}) = [f_1(\boldsymbol{x}), f_2(\boldsymbol{x}), f_3(\boldsymbol{x})] \tag{35}$$

where $f(\boldsymbol{x})$ is the vector of the three objective functions defined in the following subsection, and $\boldsymbol{x}$ is the vector of decision variables, which can be defined as follows:

$$\boldsymbol{x} = \left\{ \begin{array}{c} P_t^{G2H}, P_t^{H2G}, P_t^{BESS,ch}, P_t^{BESS,dch}, P_t^{PEV,ch}, P_t^{PEV,dch}, \\ P_t^{HVAC,h}, P_t^{HVAC,c}, P_t^{EWH}, P^{peak}, u_t^{G2H}, u_t^{H2G}, u_t^{BESS,ch}, u_t^{BESS,dch}, \\ u_t^{PEV,ch}, u_t^{PEV,dch}, u_t^{HVAC,h}, u_t^{HVAC,c}, u_t^k, on_t^k, off_t^k, u_t^{peak} \end{array} \right\} \quad \forall t = 1,2,\ldots,T \tag{36}$$

The HEMS problem considers three objective functions that reflect the economic, technical, and end-user factors, as described in the following subsection.

2.2.1. Energy cost

In an HEMS, the most typical objective function is to minimize the energy cost of daily operation by controlling the consumption of different types of appliances in an optimal manner. The objective function is expressed as follows:

$$\min f_1 = \sum_{t=1}^{T} \left\{ \Delta\tau \cdot \left(\lambda_t^{G2H} \cdot P_t^{G2H} - \lambda_t^{H2G} \cdot P_t^{H2G}\right) \right\} \tag{37}$$

where λ_t^{G2H} is the electricity tariff purchased from the utility grid at interval t and λ_t^{H2G} is the electricity tariff sold back to the utility grid at interval t.

2.2.2. Peak-to-average ratio (PAR)

The power consumption curve of a household should be as flat as possible so that utility companies can better control loads in a certain part of the distribution system (Paterakis et al., 2015). The PAR is widely used to calculate the flatness of load profiles using the following equation (Awais et al., 2018):

$$PAR = \frac{\max\left(P_t^{G2H}\right)}{\text{avg}\left(P_t^{G2H}\right)}; \forall t = 1,2,\ldots,T \tag{38}$$

However, PAR does not consider selling energy to the utility grid, and its function is nonlinear. Therefore, we considered a modified variant of PAR, which is given as follows (Alilou et al., 2020):

$$\min f_2 = \max\left(P_t^{G2H} - P_t^{H2G}\right) - \text{avg}\left(P_t^{G2H} - P_t^{H2G}\right); \forall t = 1,2,\ldots,T \tag{39}$$

To linearize the maximum function in (39), a variable (P^{peak}) is introduced as follows:

$$0 \le P^{peak} \le \overline{P}^{G2H} \tag{40}$$

$$P^{peak} \ge P_t^{G2H} - P_t^{H2G}; \forall t = 1,2,\ldots,T \tag{41}$$

$$P^{peak} \le P_t^{G2H} - P_t^{H2G} + \overline{P}^{G2H} \cdot \left(1 - u_t^{peak}\right); \forall t = 1, 2, \ldots, T \tag{42}$$

$$\sum_{t=1}^{T} \left\{u_t^{peak}\right\} = 1 \tag{43}$$

where u_t^{peak} is a binary variable representing the peak mode at interval t; u_t^{peak} is equal to 1 if $(P_t^{G2H} - P_t^{H2G})$ reaches the maximum value; otherwise, u_t^{peak} is equal to 0.

Hence, Eq. (39) can be re-written as follows:

$$\min f_2 = P^{peak} - \text{avg}\left(P_t^{G2H} - P_t^{H2G}\right); \forall t = 1, 2, \ldots, T, s.t. (40) - (43) \tag{44}$$

2.2.3. Discomfort index (DI)

To consider user behavior for load demand scheduling, a DI is introduced to calculate the difference between the baseline period (i.e., the best interval) and the scheduling intervals of controllable devices. The DI can be computed as follows (Javadi et al., 2020, 2021):

$$DI^k = \frac{1}{\delta^k} \cdot \sum_{t=1}^{T} \left| t \cdot u_t^{k,best} - t \cdot u_t^k \right|; \forall k = 1, 2, \ldots, K \tag{45}$$

where DI^k is the discomfort index for the k^{th} appliance, and $u_t^{k,best}$ is a binary parameter representing the best operation interval for the k^{th} appliance at interval t.

To preserve the MILP structure, the absolute term for the DI calculation can be easily handled using constraints, where DI^k is a positive variable as follows (Javadi et al., 2020, 2021):

$$DI^k \ge \frac{1}{\delta^k} \cdot \sum_{t=1}^{T} \left(t \cdot u_t^{k,best} - t \cdot u_t^k \right); \forall k = 1, 2, \ldots, K \tag{46}$$

$$DI^k \ge \frac{1}{\delta^k} \cdot \sum_{t=1}^{T} \left(t \cdot u_t^k - t \cdot u_t^{k,best} \right); \forall k = 1, 2, \ldots, K \tag{47}$$

Hence, DI can be included in the objective function of the proposed HEMS, as follows (Javadi et al., 2020, 2021):

$$\min f_3 = \sum_{k=1}^{K} DI^k \tag{48}$$

3. Multi-objective MILP optimization for HEMS

An MOP has at least two conflicting objective functions that are simultaneously minimized or maximized. No single optimal solution can simultaneously optimize all objective functions. In principle, the resolution of an MOP leads to a set of trade-off solutions known as Pareto optimal solutions or efficient solutions. Subsequently, decision-makers choose the "most preferred" solution from the Pareto optimal set (Aghaei et al., 2011). Several methods have been proposed to solve MOPs in the literature, such as the weighted sum method (Khaloie et al., 2020), normal boundary intersection (Khaloie et al., 2021), ε-constraint method (Khaloie et al., 2022), etc. Among these methods, the ε-constraint method is well-regarded for dealing with MOPs (Javadi et al., 2021). However, the ε-constraint method also has several limitations. First, the range of the objective functions over the efficient set is not optimized. In this regard, a lexicographic optimization approach can be used to solve this problem (Khaloie et al., 2022). Secondly, the solutions obtained using the ε-constraint approach can be the dominant solutions. This deficiency can be overcome using an augmented version of the ε-constraint approach (Khaloie et al., 2020, 2021). Therefore, we propose a multi-objective method called AUGMECON-LO, which combines the augmented ε-constraint method and lexicographic optimization to solve the MOP for the HEMS proposed in this study. Descriptions of the ε-constraint approach, lexicographic optimization, and the proposed AUGMECON-LO are presented in the following subsection.

3.1. Conventional ε-constraint method

The ε-constraint method is used to reformulate an MOP by maintaining only one objective and restricting the rest of the objectives to specified values. Generally, the ε-constraint method can be expressed as follows (Chankong & Haimes, 2008; Cohon, 2004):

$$\text{Minimize} : f_1(\boldsymbol{x}) \tag{49}$$

$$\text{Subjectto} : \begin{array}{l} f_2(\boldsymbol{x}) \le \varepsilon_2 \\ f_3(\boldsymbol{x}) \le \varepsilon_3 \\ \cdots \\ f_p(\boldsymbol{x}) \le \varepsilon_p \end{array} \tag{50}$$

In the above formulation, $\boldsymbol{x}$ is the vector of decision variables, p denotes the number of objective functions considered in the problem, and ε_p represents the upper bound of objective function f_p. We assume that all p objective functions are minimized.

Based on the payoff table, the range of each of the $(p-1)$ objective functions is defined to accurately apply the ε-constraint method. To define the payoff table for an MOP with p objective functions, the first step is to solve p single-objective subproblems. $f_i^*(\boldsymbol{x}_i^*)$ is the optimal value of f_i and $\boldsymbol{x}_i^*$ is the vector of decision variables for the single-objective subproblem of f_i. In the second step, the values of the other objective functions $f_1, f_2, \ldots, f_{i-1}, f_{i+1}, \ldots, f_p$ can be calculated using the vector of the decision solution obtained from a single-objective subproblem of f_i. The i^{th} row of the payoff tables includes $f_1(\boldsymbol{x}_i^*), f_2(\boldsymbol{x}_i^*), \ldots, f_i^*(\boldsymbol{x}_i^*), \ldots, f_p(\boldsymbol{x}_i^*)$. Accordingly, all the rows of the payoff table can be obtained as follows (Aghaei et al., 2011):

$$\Phi = \begin{bmatrix} f_1^*(\boldsymbol{x}_1^*) & \cdots & f_i(\boldsymbol{x}_1^*) & \cdots & f_p(\boldsymbol{x}_1^*) \\ \vdots & \ddots & & & \vdots \\ f_1(\boldsymbol{x}_i^*) & \cdots & f_i^*(\boldsymbol{x}_i^*) & \cdots & f_p(\boldsymbol{x}_i^*) \\ \vdots & & & \ddots & \vdots \\ f_1\left(\boldsymbol{x}_p^*\right) & \cdots & f_i\left(\boldsymbol{x}_p^*\right) & \cdots & f_p^*\left(\boldsymbol{x}_p^*\right) \end{bmatrix} \tag{51}$$

The payoff table is an $p \times p$ matrix. The j^{th} column of the payoff table includes the values obtained for the objective function f_j. The range of objective function f_j for the ε-constraint method is defined by the maximum and minimum values in the j^{th} column of the payoff table. From the payoff table, the utopia and pseudo-nadir points in the objective space can be calculated in the objective space.

The utopia point is a point outside the feasible region where all objective functions concurrently reach their minimum possible values (Aghaei et al., 2011):

$$f^U = \left[f_1^U, \ldots, f_i^U, \ldots, f_p^U\right] = \left[f_1^*(\boldsymbol{x}_1^*), \ldots, f_i^*(\boldsymbol{x}_i^*), \ldots, f_p^*\left(\boldsymbol{x}_p^*\right)\right] \tag{52}$$

Conversely, the pseudo-nadir point is defined as follows (Aghaei et al., 2011):

$$f^{SN} = \left[f_1^{SN}, \ldots, f_i^{SN}, \ldots, f_p^{SN}\right] \tag{53}$$

$$f_i^{SN} = \max\left\{f_i(\boldsymbol{x}_1^*), \ldots, f_i^*(\boldsymbol{x}_i^*), \ldots, f_i\left(\boldsymbol{x}_p^*\right)\right\}; \tag{54}$$

Accordingly, the range of each objective function can be defined using the utopia and pseudo-nadir points as follows (Aghaei et al., 2011):

$$f_i^U \le f_i(\boldsymbol{x}) \le f_i^{SN} \tag{55}$$

From the ranges defined above, the ε-constraint method divides the range of $p-1$ objective functions $f_2, \ldots, f_p$ into $q_2, \ldots, q_p$ equal intervals using $(q_2 - 1), \ldots, (q_p - 1)$ intermediate equidistant grid points, respectively. Accordingly, the total $(q_2 + 1), \ldots, (q_p + 1)$ grid points are used to parametrically vary the upper bound (ε_i) of the i^{th} objective function. Hence, the total number of subproblems to be solved is $(q_2 +$

1) × … × (q_p + 1). Assuming that the first objective function is the primary objective, the single-objective subproblems are solved sequentially as follows (Aghaei et al., 2011; Nezhad et al., 2014):

$$\text{Minimize}: f_1(\boldsymbol{x}) \tag{56}$$

$$\text{Subjectto}: f_2(\boldsymbol{x}) \le \varepsilon_{2,n_2}, \ldots, f_p(\boldsymbol{x}) \le \varepsilon_{p,n_p} \tag{57}$$

$$\varepsilon_{2,n_2} = f_2^{SN} - \left(\frac{f_2^{SN} - f_2^{U}}{q_2}\right) \times n_2; n_2 = 0, 1, \ldots, q_2 \tag{58}$$

$$\varepsilon_{2,n_p} = f_p^{SN} - \left(\frac{f_p^{SN} - f_p^{U}}{q_p}\right) \times n_p; n_p = 0, 1, \ldots, q_p \tag{59}$$

In the ε-constraint method, one Pareto optimal solution can be found once each single-objective subproblem is solved. Some of these single-objective subproblems may contain infeasible solution spaces that are discarded.

3.2. Augmented ε-constraint method with lexicographic optimization (AUGMECON-LO)

The original payoff table defined above has the disadvantage that the solutions obtained from single-objective subproblems may not be Pareto optimal solutions or efficient solutions (Mavrotas, 2009). To overcome this situation, lexicographic optimization can be used to determine the payoff table using only Pareto optimal solutions. Mathematically, the lexicographic optimization process of a series of objective functions is to optimize the first objective function, and then the remaining possible alternative optima are optimized for the second objective function. In lexicographic optimization, the first objective function (or objective function with a higher priority) is initially optimized, assuming that $\min f_1 = f_1^*(\boldsymbol{x}_1^*)$ is obtained. Subsequently, the second objective function is optimized by adding the constraint $f_1 = f_1^*(\boldsymbol{x}_1^*)$ to maintain the optimal solution of the first optimization, assuming that the $\min f_2 = f_2^*(\boldsymbol{x}_2^*)$ is obtained. Subsequently, the third objective function is optimized by adding the constraints $f_1 = f_1^*(\boldsymbol{x}_1^*)$ and $f_2 = f_2^*(\boldsymbol{x}_2^*)$ to maintain the

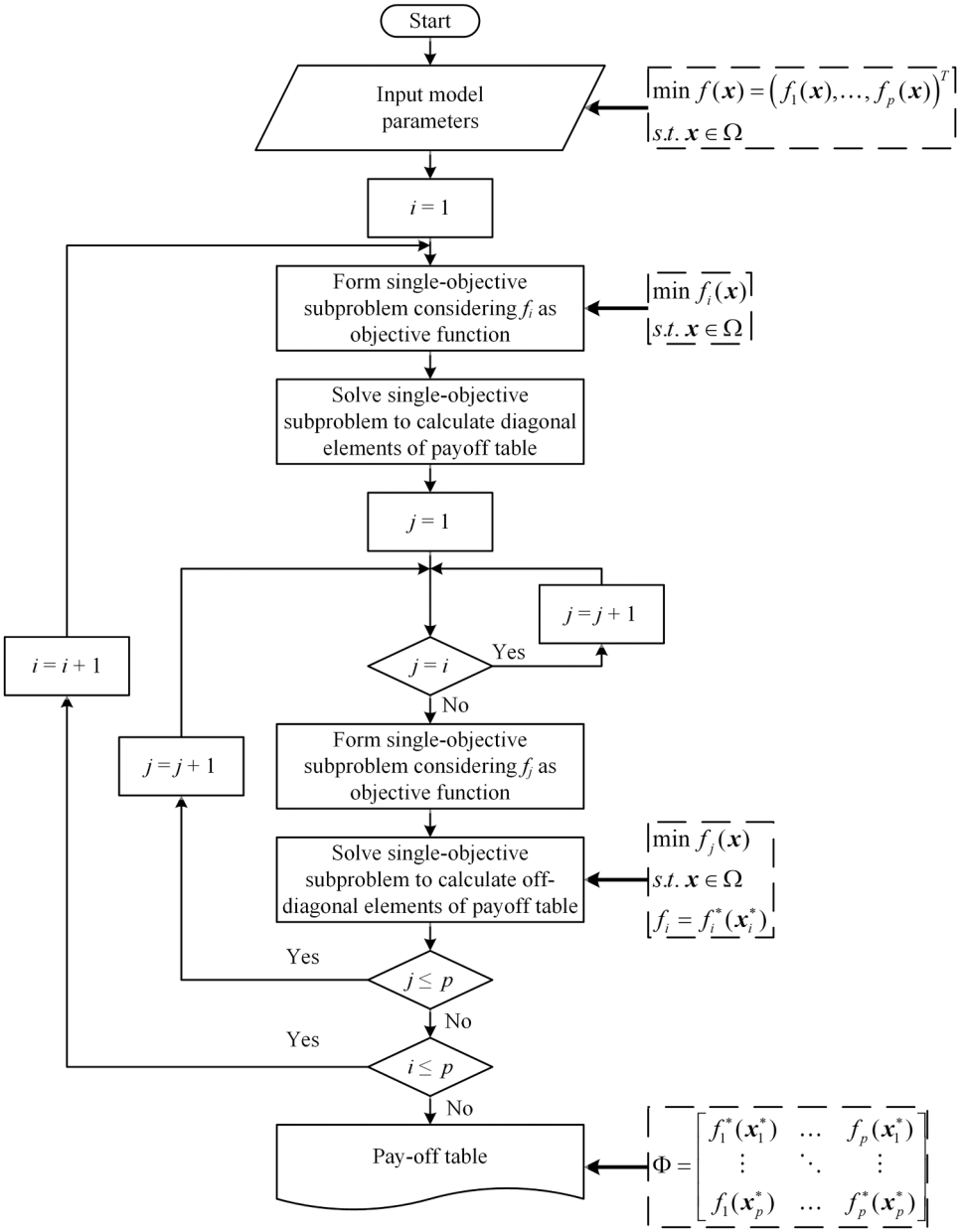

Fig. 2. Flowchart of the lexicographic optimization for payoff table calculation.

previous optimal solutions until the objective functions are all optimized (Mavrotas & Florios, 2013). Fig. 2 illustrates the flowchart of the lexicographic optimization.

As mentioned, the solutions obtained using the ε-constraint method may not be effective. The AUGMECON-LO method transforms the inequality constraints of the objective functions into equality constraints by explicitly integrating the appropriate slack or surplus variables. The formulation of an MOP based on the AUGMECON-LO method is as follows (Mavrotas, 2009):

$$\text{Minimize}: f_1(\boldsymbol{x}) - eps \times \left(s_2 / r_2 + s_3 / r_3 + \ldots + s_p / r_p\right) \tag{60}$$

$$\text{Subjectto}: \begin{array}{c} f_2(\boldsymbol{x}) + s_2 = \varepsilon_2 \\ f_3(\boldsymbol{x}) + s_3 = \varepsilon_3 \\ \cdots \\ f_p(\boldsymbol{x}) + s_p = \varepsilon_p \\ s_1, s_2, \ldots, s_p \in R^+ \\ \boldsymbol{x} \in \Omega \end{array} \tag{61}$$

where $s_2, s_3, \ldots, s_p$ are slack variables, *eps* is an adequately small number (usually between 10^{-3} and 10^{-6}), r_i is the range of the i^{th} objective function as defined from the payoff table (i.e., $r_i = f_i^{SN} - f_i^U$), and Ω denotes the feasible region. Based on this method, the slack variable s_i of objective function f_i is scaled to the range of the first objective function f_1. Fig. 3 depicts the conceptual flowchart of the proposed AUGMECON-LO.

3.3. Decision-making method

It is vital to extract the compromise solution from the Pareto optimal set. To this end, a decision-making method based on fuzzy set theory is proposed to define the compromise solution from the trade-off curve. Each objective function j of the i^{th} solution is assigned a membership function μ_{ij}, which can be expressed as follows (Huy et al., 2022):

$$\mu_{ij} = \begin{cases} 1 & \text{if} f_{ij} \le \min\left(f_j\right) \\ \dfrac{\max\left(f_j\right) - f_{ij}}{\max\left(f_j\right) - \min\left(f_j\right)} & \text{if} \min\left(f_j\right) \le f_{ij} \le \max\left(f_j\right) \\ 0 & \text{if} f_{ij} \ge \max\left(f_j\right) \end{cases} \tag{62}$$

where $\min(f_j)$ and $\max(f_j)$ denote the minimum and maximum values of the j^{th} objective function, respectively. Fig. 4 shows a graphical representation of the fuzzy membership function.

The higher the membership function, the more satisfying the solution. The normalized membership function for each non-dominated solution can be computed as follows (Huy et al., 2022):

$$\mu_i = \frac{\sum_{j=1}^{n_{obj}} \mu_{ij}}{\sum_{i=1}^{n_{pf}} \sum_{j=1}^{n_{obj}} \mu_{ij}} \tag{63}$$

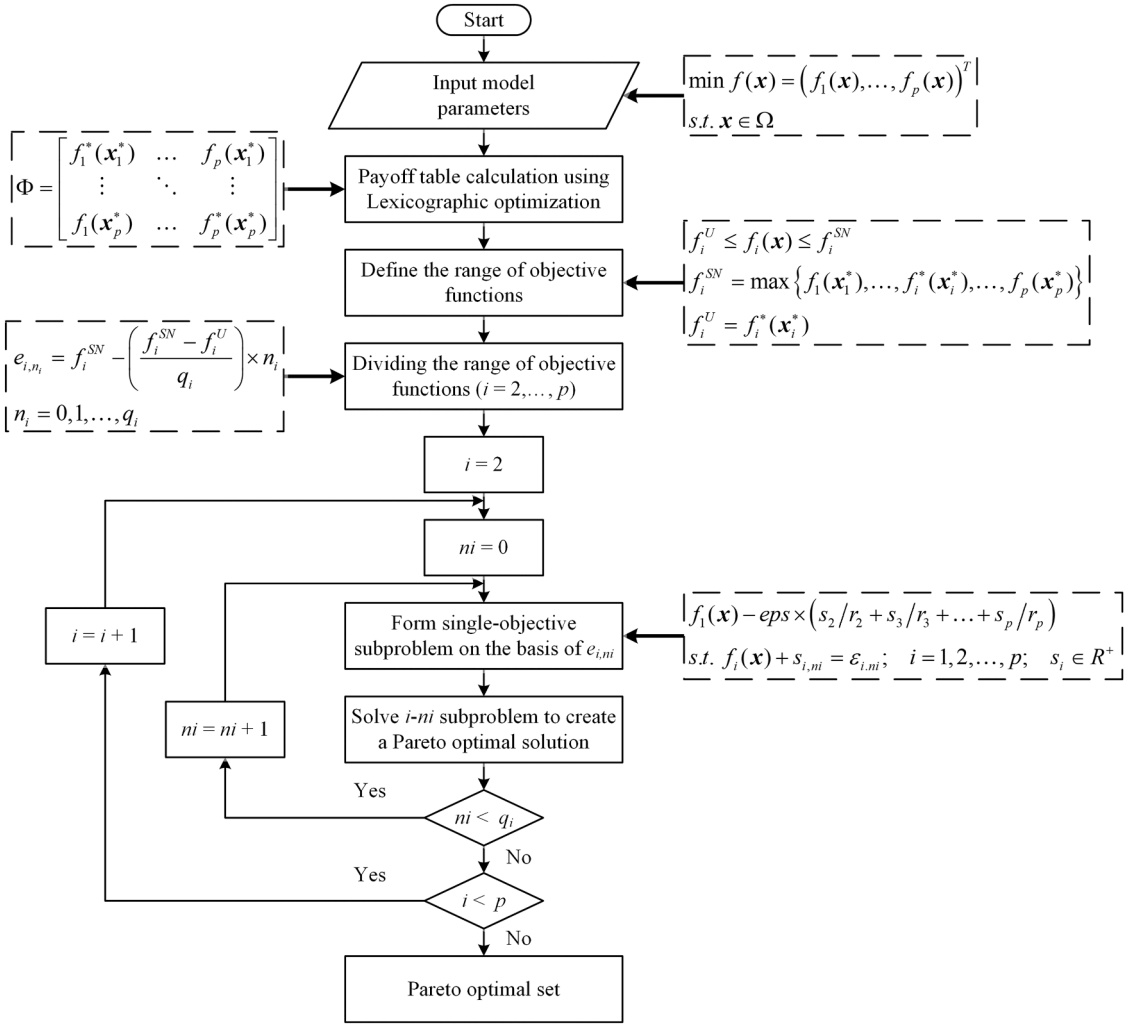

Fig. 3. Flowchart of the proposed AUGMECON-LO.

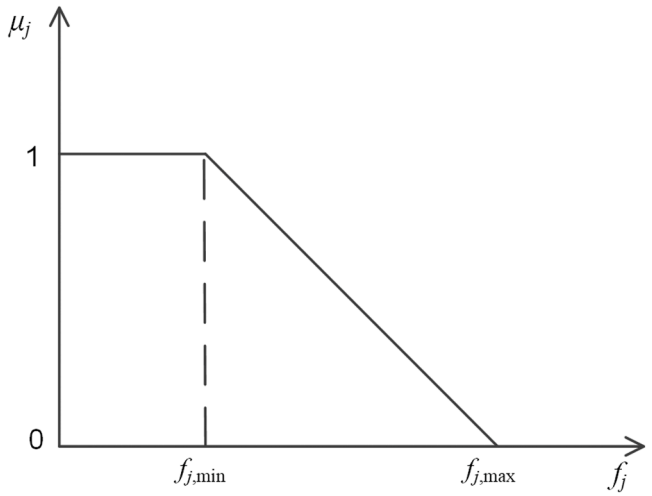

Fig. 4. Fuzzy membership function.

where n_{obj} represents the number of objective functions and n_{pf} is the number of non-dominated solutions. The compromise solution is that with the largest normalized membership function value (μ_i).

In this study, the proposed AUGMECON-LO is applied to a multi-objective HEMS optimization problem. In this regard, minimization of the energy cost is considered the main objective function for residential users. Other objective functions, including PAR and DI, are treated as constraints in the AUGMECON-LO method. An overall flowchart of the proposed methodology for the multi-objective HEMS framework is shown in Fig. 5.

4. Simulation results

In this section, the proposed multi-objective HEMS paradigm is validated using various simulation results. This study investigates the

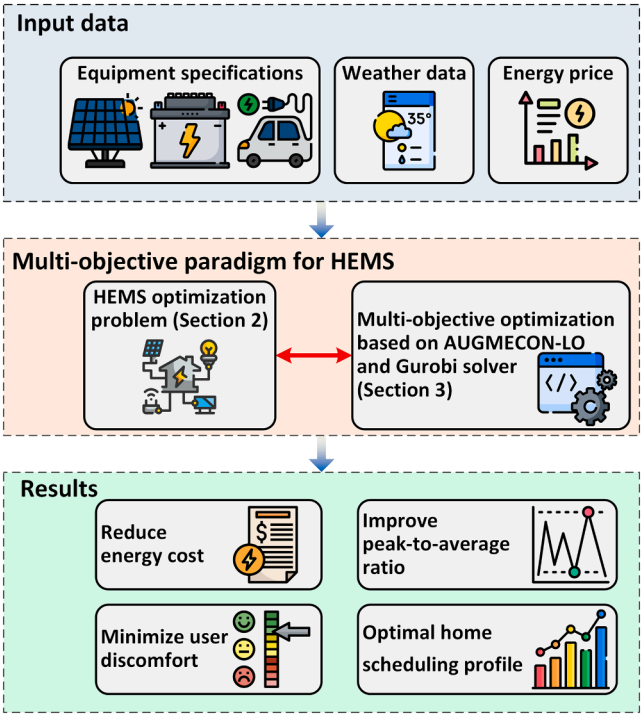

Fig. 5. Flowchart of the proposed methodology for multi-objective HEMS framework.

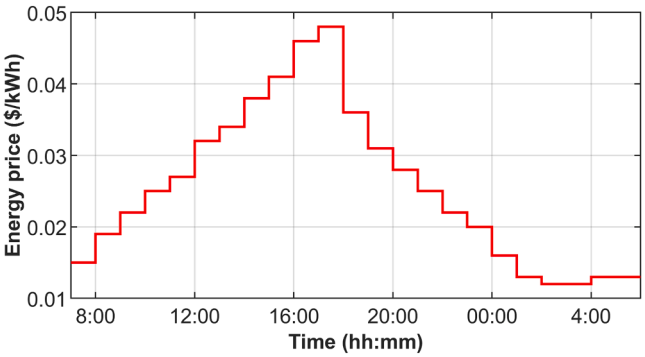

Fig. 6. Day-ahead hourly price under study.

Table 2
Data of utility grid and solar PV system.

Parameter	Value
$\overline{P}^{G2H}/\overline{P}^{H2G}$	10/4 kW
$\overline{P}^{PV}$	1 kW
η^{PV}	0.167

HEMS model by using both deterministic and stochastic models. The deterministic model considers day-ahead data for solar irradiation, ambient temperature, and the initial SOE of the PEV. The stochastic model treats these factors as uncertain parameters. The simulations are performed over a 24 h time horizon with a time step of 30 min (7:00–6:30 h), resulting in 48 intervals in the daily scheduling process. The MILP formulation of the HEMS system is developed in Python and solved using the Gurobi optimizer. The simulations are executed on a 64-bit Intel (R) Core(TM) i7-7700 CPU @ 3.6 GHz with 16-GB RAM.

4.1. Deterministic model

4.1.1. Input data

In this study, a typical smart home is considered to evaluate the proposed model. The day-ahead electricity tariffs of a typical day in July 2020 are taken from the data of the Commonwealth Edison Company (ComEd's Hourly Pricing Program, 2022), as shown in Fig. 6. It is assumed that the selling price is equal to the purchase price. Table 2 presents the data for the utility grid and the solar PV system. The

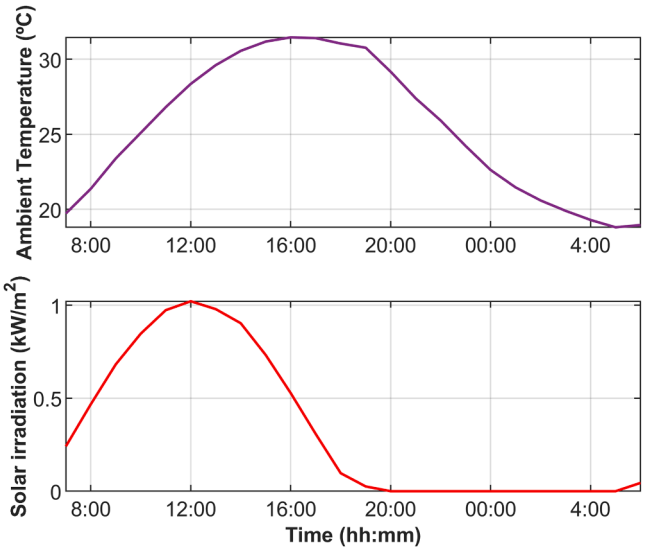

Fig. 7. Ambient temperature and solar irradiance under study.

Table 3
Data of controllable and non-controllable appliances.

Type	Appliance	P^k	δ^k	Allowable operation range	Best operation range
Controllable appliance	Dishwasher	2.5	4	2 – 20	6 – 9
	Washing machine	3	3	3 – 10	6 – 8
	Spin dryer	2.5	2	12 – 22	14 – 15
	Cooker hub	3	1	3 – 4	4 – 4
	Microwave	1.7	1	3 – 4	4 – 4
	Laptop	0.1	4	20 – 34	24 – 27
	Vacuum cleaner	1.2	1	5 – 20	6 – 6
Non-controllable appliance	Refrigerator	0.35	48	1 – 48	1 – 48
	Television	0.1	12	22 – 33	22 – 33
	Light	0.1	12	12 – 35	12 – 35

Table 4
Data of BESS and PEV.

BESS		PEV	
Parameter	Value	Parameter	Value
$\overline{\varepsilon}^{BESS}$	5 kWh	$\overline{\varepsilon}^{PEV}$	22 kWh
$\overline{P}^{BESS,ch}/\overline{P}^{BESS,dch}$	2 kW/ 2 kW	$\overline{P}^{PEV,ch}/\overline{P}^{PEV,dch}$	3 kW/ 3 kW
η^{BESS}	0.98	η^{PEV}	0.98
DOD^{BESS}	0.70	DOD^{PEV}	0.80

Table 5
Data of HVAC and EWH systems.

HVAC		EWH	
Parameter	Value	Parameter	Value
$\overline{P}^{HVAC,h}/\overline{P}^{HVAC,c}$	2 kW/ 2kW	$\overline{P}^{EWH}$	2.1 kW
COP	1.20	$C^{w,h}$	1.52 kWh/°C
$\theta^{HVAC,sp}$	23°C	$R^{w,h}$	863.40°C/kW
$\overline{\theta}^{in}$	23.5°C	$\overline{v}^{EWH}$	50 Gal
$\underline{\theta}^{in}$	22.5°C	η^{EWH}	0.90
M	1778.40 kg	$\theta^{EWH,sp}$	45°C
C_p	1.01 kJ/(kg·°C)	$\overline{\theta}^{w,h}$	60°C
R	$3.20{\cdot}10^{-6}$ J/°C	$\underline{\theta}^{w,h}$	40°C
		$\theta^{w,c}$	10°C

maximum powers that could be purchased and sold between the home and utility grids are 10 and 4 kW, respectively. The proposed HEMS is equipped with a small-scale solar PV system of 1 kW. Solar irradiance and ambient temperature are extracted from (European Commission, 2022) for a typical day in 2020 in Madrid (Spain), as depicted in Fig. 7. Table 3 lists the data for non-controllable and controllable appliances (Javadi et al., 2020, 2021; Rezaee Jordehi, 2020). Moreover, the HEMS has a BESS Li-ion system and a Renault Zoe electric car as the PEV (Shafie-Khah & Siano, 2018), which are listed in Table 4. For simplicity, the PEV is assumed to arrive and connect to the HEMS at 19:30 with an initial SOE of 50%, and to depart at 6:30. Table 5 provides the data for thermostatically controlled appliances, including HVAC and EWH systems, which are obtained from (Paterakis et al., 2015; Tostado-Véliz et al., 2021). Fig. 8 also depicts the hot water consumption, as described by (Rosin et al., 2017; Tostado-Véliz et al., 2021).

Fig. 9 presents the base-load profile of the investigated home before conducting the HEMS scheduling. In the base-load paradigm, it is assumed that BESS is not considered. All controllable appliances are operated at the user's preferred time. The PEV is charged as soon as it arrived home until its battery reaches fully capacity; therefore, the V2H mode is not considered. The HVAC system is operated to maintain the temperature at a set point. The EWH operates at the rated power and only changes the operating status when the hot water temperature is not within the allowable range. Without HEMS scheduling and BESS, the

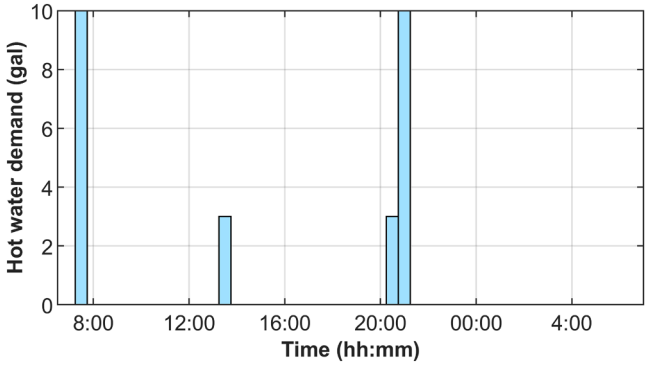

Fig. 8. Hot water consumption.

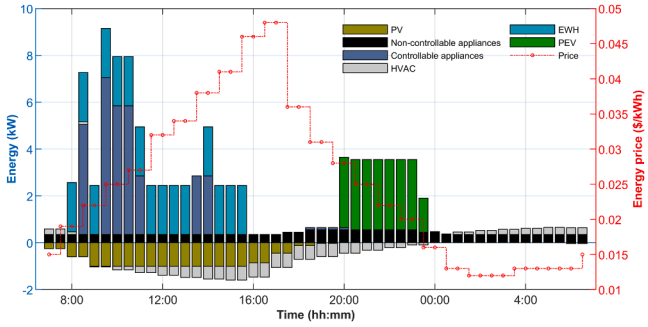

Fig. 9. Base-load profile.

Table 6
Results for single-objective subproblems.

Subproblem	Energy cost	PAR	DI
Subproblem 1: Energy cost minimization	0.6041	4.0918	18
Subproblem 2: PAR minimization	1.1283	0	29
Subproblem 3: DI minimization	0.9837	2.2317	0

home cannot store excess energy from the solar PV. Consequently, the base-load profile yields an energy cost of 1.3146, PAR of 3.0472, and the minimum DI value. The variations in the load profile and objective function values are discussed and analyzed for evaluating the effectiveness of the proposed model in the following subsection.

4.1.2. *Results for single-objective optimization*

In this case, the energy cost, PAR, and DI objectives are individually minimized to investigate the contradictory nature of the various objectives. The values of the objective functions in the three single-objective subproblems are presented in Table 6 and Fig. 10. The minimum value of one objective may lead to a high value of another objective. Specifically, the energy cost and PAR are conflicting objective functions because the minimum point of energy cost is obtained at the maximum point of the PAR, and vice versa.

The scheduling profile of the HEMS for each single-objective optimization subproblem is presented in Fig. 11, clearly illustrating their contradictory nature. As shown in Fig. 11, when the energy cost is minimized, most home loads are shifted to operate at intervals of low electricity tariffs. This leads to an imbalance in household load profiles, which significantly increases the PAR value. Furthermore, controllable devices may not operate at the preferred intervals of user demand; therefore, the DI value is very high. In the subproblem of PAR minimization, energy from the grid is overpurchased to flatten the load profile of the household. In this case, the HEMS does not sell energy to the grid at any given interval and V2H is not utilized. As a result, energy cost increases considerably. In subproblem 3, the HEMS operates devices

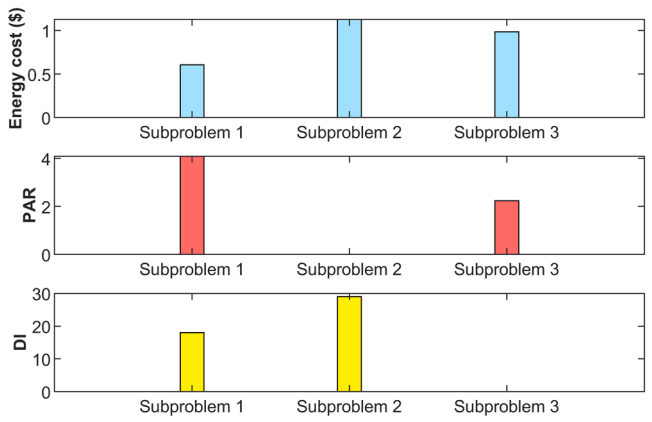

Fig. 10. Value of each objective function for single-objective subproblems.

based on user behavior to minimize the DI objective; thus, the values of the other objectives are not fully considered. Hence, the HEMS problem should be formulated as a multi-objective rather than a single-objective problem.

4.1.3. Results for multi-objective optimization

The main purpose of the proposed multi-objective paradigm for HEMS is to simultaneously minimize the energy cost, PAR, and DI. Multi-objective optimization of HEMS is performed by applying the proposed AUGMECON-LO. A detailed description of the application of the proposed AUGMECON-LO is presented herein.

From Table 6, the original payoff table (Φ_1) can be obtained based on the single-objective optimization subproblems as follows:

$$\Phi_1 = \begin{bmatrix} 0.6041 & 4.0918 & 18 \\ 1.1283 & 0 & 29 \\ 0.9837 & 2.2317 & 0 \end{bmatrix}$$

The values in the first column refer to the objective function f_1 (i.e., energy cost). The values in the second and third columns refer to objective functions f_2 (PAR) and f_3 (DI), respectively. The utopia point ($f^U = [0.6041, 0, 0]$) includes the minimum possible values for all objective functions, which lie on the main diagonal of payoff table Φ_1. Meanwhile, the pseudo-Nadir point ($f^{SN} = [1.1283, 4.0918, 29]$) contains the maximum values in each column of the payoff table Φ_1.

To guarantee the Pareto optimality of the individual optima, the proposed AUGMECON-LO uses lexicographic optimization in the construction of the payoff table Φ_2, as presented in Fig. 2. Hence, the payoff table Φ_2 is as follows:

$$\Phi_2 = \begin{bmatrix} 0.6041 & 4.0918 & 18 \\ 1.1018 & 0 & 15 \\ 0.6702 & 3.1670 & 0 \end{bmatrix}$$

It can be observed that the values of the second row of the payoff table Φ_2 are better than those of the payoff table Φ_1. By comparing the payoff tables Φ_1 and Φ_2, the range of the objective function f_2 is preserved; however, a narrower range is obtained for the objective function f_3. From the payoff table, the two ranges of PAR and DI objectives are divided into six equal intervals (i.e., $q_2 = 6$ and $q_3 = 6$), which means that seven grid points are used for each range of the two objective functions, and 49 optimization subproblems are solved to obtain the Pareto optimal set. Two out of the 49 subproblems with infeasible solution spaces are discarded, resulting in 47 obtained Pareto optimal solutions.

A graphical representation of the Pareto front is depicted in Fig. 12, which shows that the proposed AUGMECON-LO provides a wide range of Pareto optimal solutions. With the obtained Pareto optimal set, the decision-making method is used to select the optimal compromise solution. To this end, the normalized membership function value is computed for each Pareto optimal solution, which indicates the satisfaction of each solution for all the objective functions. The higher the normalized membership function value, the more the Pareto optimal solution is compromised. The compromise solution is also highlighted in Fig. 12, and its optimal results are presented in Table 7. The compromise solution yields an energy cost of 0.6841, a PAR of 1.3639, and a DI of 0. As a result, the energy costs and PAR are reduced by 47.96% and 55.24%, respectively, compared to the base-load profile, whereas the DI reaches the minimum value. Moreover, a compromise solution is obtained between the utopia point and pseudo-nadir point. Hence, the proposed method achieves a compromise solution for all considered objective functions.

The scheduling profile of the HEMS after multi-objective optimization is shown in Fig. 13. All controllable appliances complete their assigned tasks efficiently within the defined operation period, and the uninterrupted operation of these appliances is guaranteed. Controllable appliances operate mainly when the solar power generation is high, or electricity tariffs are low. Consequently, solar PV power generation is primarily used for household power consumption and BESS charging. The surplus energy can then be sold back to the grid when the household power consumption is low and the BESS is fully charged. In particular, a total energy of 7.1717 kW of the solar PV system is provided for self-consumption and BESS, accounting for 76.79% of the total solar power output (9.3393 kW). Meanwhile, the amount of energy injected into the grid from the solar PV system is only 2.1676 kW (23.21%). Therefore, the proposed HEMS scheduling can avoid wasting the energy generated from the solar PV system.

The SOE and state of charge (SOC) of BESS over the scheduling intervals are shown in Fig. 14. In the morning and midday, the charging mode of the BESS is activated to take advantage of the high power generated by the solar PV and the low peak of the electricity tariffs, as shown in Fig. 14. The BESS is discharged to supply energy when the power consumed by the home load reached a high peak. As the BESS can store a limited amount of energy, its SOE is preserved after a full charge from 11:30 to 15:00 h. At the high peak of electricity tariffs from 15:30 to 17:00, this stored energy is not only used to meet the total energy consumption of the household load, but also sold to the grid to maximize the economic benefits of the prosumer. Subsequently, BESS is temporarily inactive until the next day. During operation, the SOE of the BES is always within its depth of discharge and maximum capacity, as set by the HEMS.

Fig. 15 shows the SOE and SOC of the PEV during the scheduling interval. In this case, the PEV arrives at home and connects to the HEMS at 19:30 h; however, the PEV charging is delayed until the end of the peak period. When the stored energy of the BESS is no longer available, the remaining energy of the PEV is used to supply the load demand and sell back to the grid, owing to its V2H capability. As shown in Fig. 15, the PEV is charged only during intervals of low electricity tariffs to minimize the charging costs. Although the total charging power increases from 11.2245 to 17.9592 kW (base-load profile) owing to the exploitation of the V2H capability, the charging cost decreases from $0.2546 to $0.2296. Furthermore, the PEV releases a total of 6.4680 kW through the V2H mode, contributing to a lower energy cost and PAR. With this defined scheduling plan, the PEV is guaranteed to be fully charged at the time of departure to increase the consumer satisfaction.

Figs. 16 and 17 depict the scheduling profiles for the HVAC and EWH, respectively. As observed in Fig. 16, the indoor temperature should be kept between 22.5 and 23.5°C based on the user preference. When the outdoor temperature increases from 11:00 to 23:30 h, the HVAC system is operated in the cooling mode. When the outdoor temperature is low from 0:00 to 6:30 h, the HVAC system is operated in heating mode. Therefore, the indoor temperature is always kept within the allowable limits [22.5–23.5°C]. The power consumption of the HVAC system is lower during on-peak electricity tariffs (between 15:30 and 17:00). Although the rated power of HVAC is 2 kW, the power consumption of HVAC to be optimized for cost reduction is

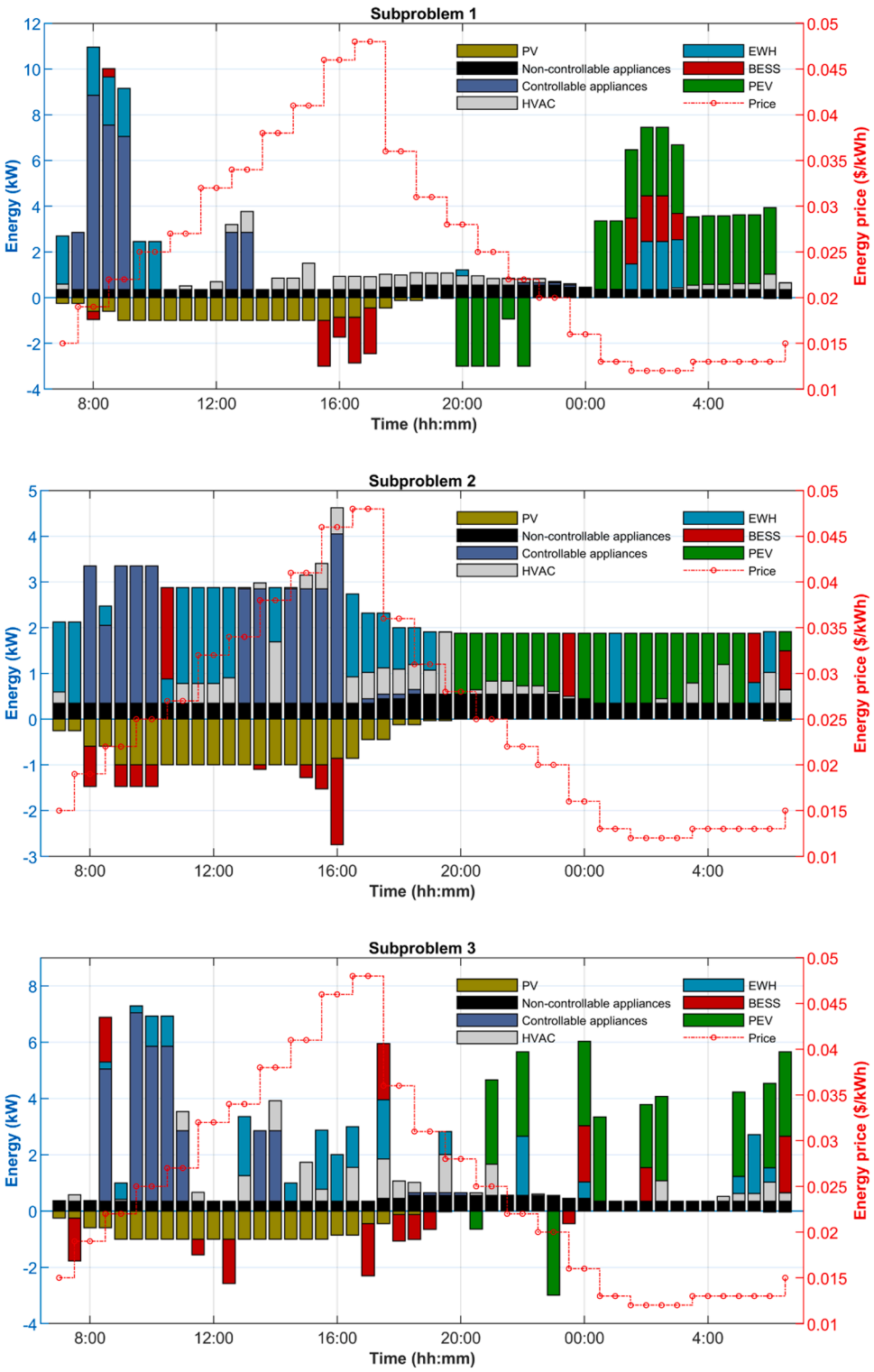

Fig. 11. Scheduling profile for single-objective optimization subproblems. Negative energy indicates "energy to HEMS" direction from solar PV, BESS, and PEV.

approximately less than 1 kW. This is much more beneficial than simply turning the commitment of the HVAC system into a fixed power mode. It is deduced that employing the proposed HEMS paradigm curtails a significant portion of the total daily power consumption of the HVAC system from 7.6254 kW (base-load profile) to 6.3559 kW, resulting in a 16.65% reduction in power consumption. Moreover, the average daily indoor temperature is 23.14°C, indicating that the HVAC system is efficiently operated to provide relatively high thermal comfort to the user.

As shown in Fig. 17, when home users use hot water for showering and other daily requirements, the HEMS controls the EWH operation at certain intervals with optimal power consumption to maintain the hot water temperature within 40 and 60°C. When the outdoor temperature increases in the afternoon, the EWH is mostly off, but the hot water temperature remains within its limits. In the early morning, the low outdoor temperature affects the hot-water temperature in the tank.

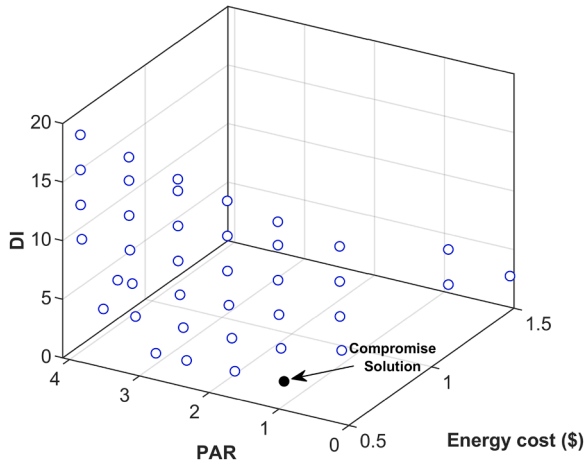

Fig. 12. Pareto optimal front for multi-objective HEMS optimization.

Therefore, EWH increases the hot water temperature before the home demand. After optimization, the total energy consumption of EWH is reduced from 15.75 to 10.0371 kW, which corresponds to a reduction of 36.27%. The average daily hot water temperature is 43°C, which is close to the initial set point of 45°C (see Fig. 17). Thus, a reduction in the EWH power consumption for EWH is achieved without compromising thermal comfort.

Fig. 18 depicts the energy traded between the HEMS and the utility grid. The load profile is relatively flat in the morning. During off-peak electricity tariffs, the HEMS purchases the required energy from the grid to supply home loads and charged the BESS and PEV. During on-peak electricity tariffs, surplus power is injected back into the grid to create profit for the prosumer. Furthermore, the amount of power transacted between the HEMS and the grid during each period is less than the maximum power limit. The total energy of G2H is 50.8435 kW, which represents a slight increase of 1.67% compared to the base load profile (50.0107 kW). The HEMS model draws energy from the grid and stores energy in the BESS during off-peak intervals. Moreover, the total energy of H2G is 7.3238 kW, which is much higher than that of the base load profile (0 kW).

In summary, the proposed HEMS successfully coordinates the operation of home electrical devices to optimize predefined objective functions while satisfying user demand for home loads. The proposed HEMS model provides intelligent charging and discharging decisions for BESS and PEV. Based on self-generation from solar PV systems and storage capacity from BESS and PEV, HEMS can reasonably adjust the energy of G2H and H2G to reduce the energy cost and PAR simultaneously, especially during high demand intervals. Moreover, thermostatically controlled appliances, such as HVAC and EWH systems, are precisely fine-tuned in the optimal control strategy to meet the user requirements for energy cost reduction and thermal comfort. Considerable reductions in the energy cost and PAR are achieved by applying the proposed HEMS paradigm. It is worth mentioning that these reductions are achieved without sacrificing user comfort. For utility grids, PAR reduction may limit peak load effects and avoid unexpected power outages at high peak demand. As a result, with the proposed HEMS, residential end users can effectively participate in the demand response program that benefits both the grid and user.

Table 7
Results for multi-objective optimization.

Objective	Utopia	Pseudo-Nadir	Multi-objective results
Energy cost	0.6041	1.1283	0.6841
PAR	0	4.0918	1.3639
DI	0	29	0

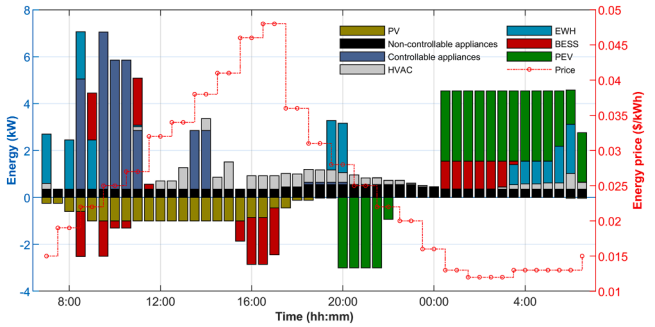

Fig. 13. Scheduling profile for the multi-objective optimization problem.

4.1.4. Analysis of the impact of storage capacity

In this section, the impact of the storage capacity on the scheduling profile of an HEMS is discussed. Therefore, three expansion cases are performed and analyzed as follows:

Case 1: PEV is assumed to be unable to provide V2H capability. This is a common case, as the V2H capability is not available for all PEV. Hence, BESS is the only device that can provide storage capacity for HEMS.
Case 2: Assume that the BESS is not integrated into the HEMS. Accordingly, only the PEV can provide storage capacity using their V2H capability.
Case 3: The PEV cannot provide V2H capability and the BESS is not integrated. In this regard, the HEMS under study does not have any energy storage capacity.

Table 8 provides a comparison between the comprehensive HEMS in Section 4.1.3, and the three expansion cases in terms of the energy cost, PAR, and DI objectives. The scheduling profiles of the expansion cases are shown in Fig. 19. As shown in Table 8, a comprehensive HEMS model containing both BESS and V2H yields the lowest energy cost, PAR, and DI values. In Case 1, the energy cost increases compared with the comprehensive HEMS model. The other objectives, including PAR and DI, are similar to those of the comprehensive HEMS model. With the exception of the PEV not participating in the 20:00–22:00 h scheduling period, the scheduling profile of Case 1 is relatively similar to that shown in Fig. 13. HEMS without V2H may still be beneficial because the BESS can provide adequate storage capacity. For Cases 2 and 3, when the BESS is not installed, the values of the energy cost, PAR, and DI increase considerably compared to the comprehensive HEMS model. In particular, the energy cost, PAR, and DI in Case 2 are 0.7873, 1.4482, and 4, respectively, which are higher than those in Case 1 (i.e., 0.7549, 1.3658, and 0, respectively). Meanwhile, HEMS without storage capacity obtains

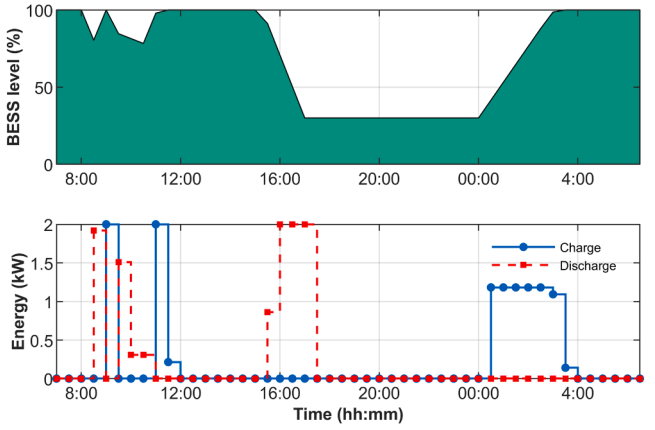

Fig. 14. SOE and SOC of the BESS.

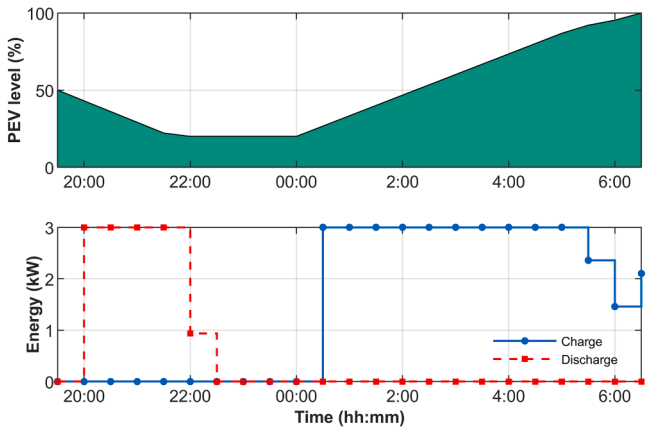

Fig. 15. SOE and SOC of the PEV.

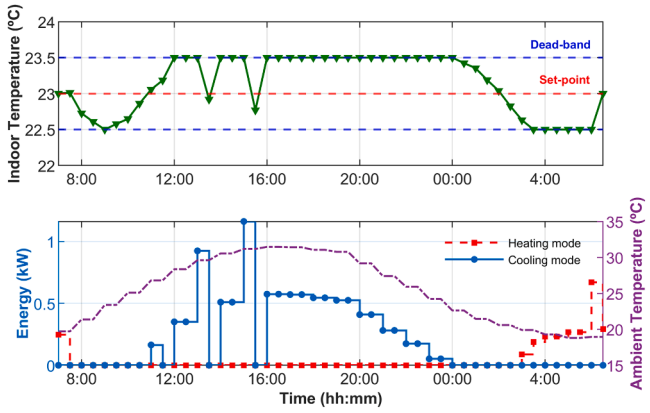

Fig. 16. Scheduling profile of the HVAC system.

objective function values of 0.8549, 1.4619, and 5, respectively, which are the highest values compared to the other cases. This is explained by the fact that the HEMS loses flexible energy storage from the BESS in Cases 2 and 3. The differences in the PAR and DI values in Cases 2 and 3 are not significant. As shown in Fig. 19, the scheduling profiles of Cases 2 and 3 are also not significantly different. It can be concluded that BESS has a more significant influence on home scheduling than the PEV.

With the unavailability of BESS, the energy generated from the solar PV system is only used for home loads, and the surplus is sold to the grid at any electricity tariff. Moreover, HEMS cannot store the energy drawn from the grid at intervals of low tariffs and uses this amount of energy for

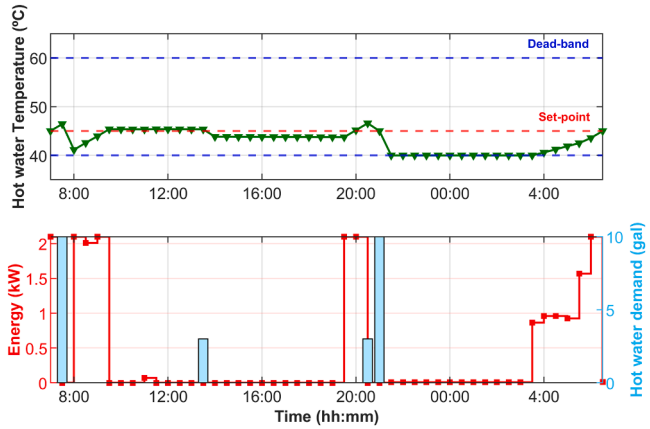

Fig. 17. Scheduling profile of the EWH system.

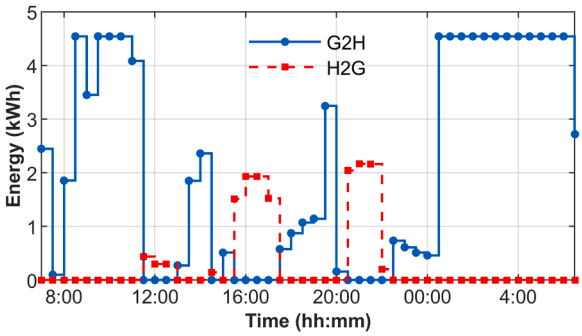

Fig. 18. Traded energy between HEMS and the utility grid.

on-peak tariffs, as scheduled in a comprehensive HEMS model. Although there is a certain storage capacity for the PEV in Case 2, the PEV is only available at certain times of the day and should be fully charged at its departure time. This leads to very limited utilization of V2H compared with BESS. In contrast to the PEV, BESS provides a flexible storage capacity throughout the scheduling process, especially during intervals when the solar PV system generates a large power output. Therefore, a BESS is an essential device to be installed in a typical smart home.

4.1.5. *Analysis of the impact of solar PV sizing*

In this section, various simulations are performed to analyze the impact of solar PV sizing on HEMS scheduling. To perform this analysis, it is assumed that the peak power of the solar PV system is changed from 1 to 3 kW with a step size of 0.5. Table 9 shows the values of the energy cost, PAR, and DI objectives for different peak powers of the solar PV systems. From Table 9, the DI values are all zero for different solar PV sizing, which provides the maximum user satisfaction for this study. Moreover, it is clear that the energy cost and PAR objectives are enhanced as the size of the PV system increases. The energy cost is reduced by up to 73.75%, whereas the PAR improves by up to 48.02% as the solar PV peak power increases from 1 to 3 kW. This can be observed more clearly in Table 9, which shows the total energy exchange between the HEMS and utility grid. The increased output power from the solar PV system contributes a large part to supplying home loads in the middle of the day. When the solar PV peak power reaches 3 kW, the total amount of purchased energy is remarkably reduced by 25.85% (from 50.8435 to 37.6983 kW) compared with the case of 1 kW of peak power. Accordingly, the load pattern is also noticeably flattened when the solar PV system operates. It can be concluded that increasing the solar PV sizing is of great benefit to HEMS scheduling in terms of economic and technical aspects.

4.1.6. *Comparison with other methods*

In general, the mathematical model of the proposed HEMS can be solved using MOEAs, such as the non-dominated sorting genetic algorithm II (NSGA-II) (Deb et al., 2002), multi-objective particle swarm optimization (MOPSO) (Coello et al., 2004), and multi-objective search group algorithm (MOSGA) (Huy et al., 2022). Such MOEAs are well-known and have been applied to various multi-objective engineering optimization problems. In this section, the proposed AUGMECON-LO is compared with the NSGA-II, MOPSO, and MOSGA to

Table 8
Comparative results between the comprehensive HEMS and three expansion cases.

Case	Energy cost	PAR	DI
Comprehensive HEMS	0.6841	1.3639	0
Case 1 – HEMS without V2H	0.7549	1.3658	0
Case 2 – HEMS without BESSS	0.7873	1.4482	4
Case 3 – HEMS without storage capacity	0.8549	1.4619	5

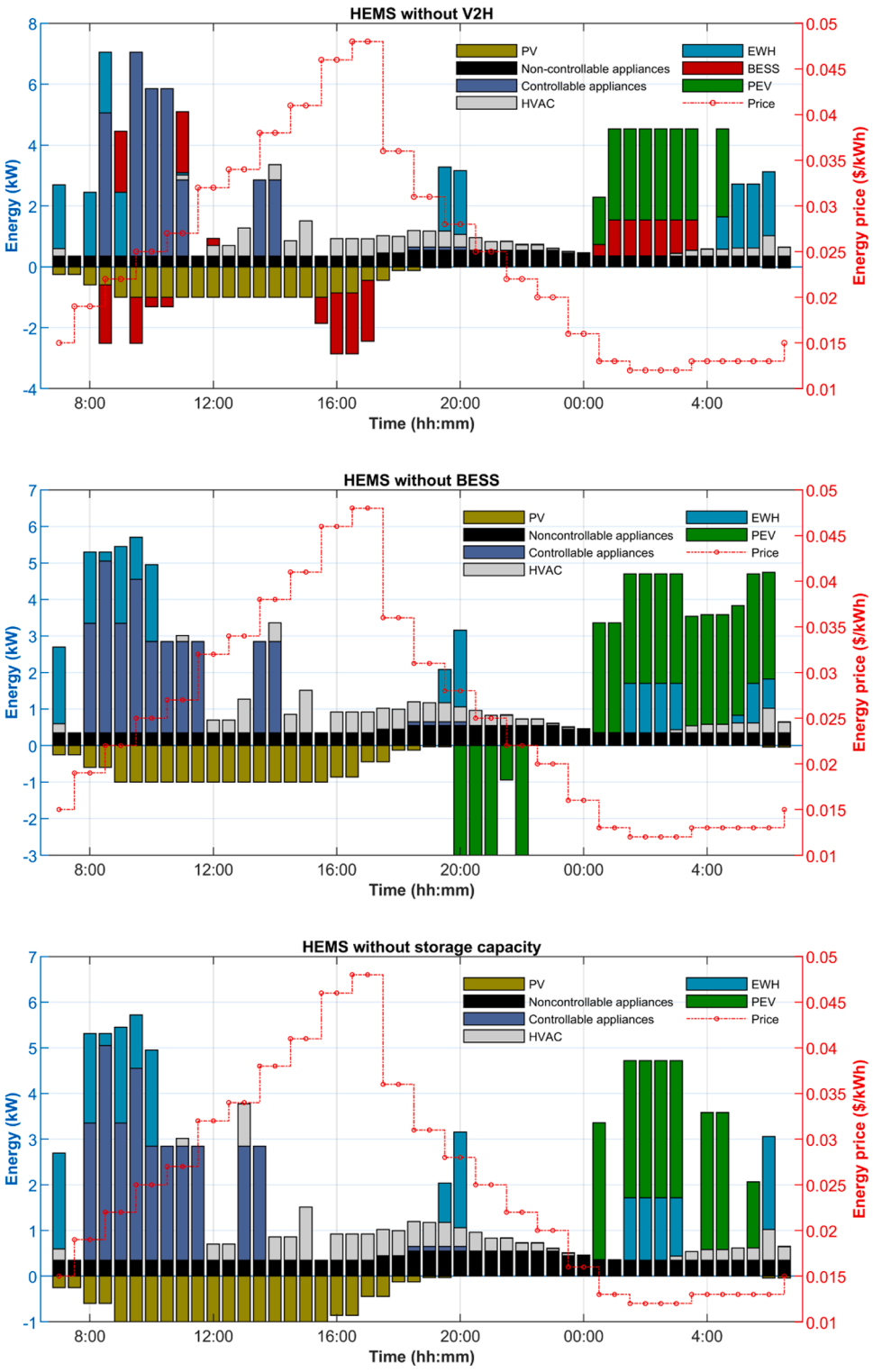

Fig. 19. Scheduling profile for three expansion cases.

solve the multi-objective formulation of the HEMS under study. A comparison of the compromise solutions for the considered cases is presented in Table 10. To obtain feasible solutions for the optimization considered in this study, NSGA-II, MOPSO, and MOSGA are implemented with a population size of 500 and a maximum iteration count of 10000. The other parameter settings of these MOEAs are similar to those in (Huy et al., 2022).

The compromise solutions achieved by the proposed AUGMECON-LO dominates those achieved by the other MOEAs in all three objective functions for the cases under study. For the comprehensive HEMS model, AUGMECON-LO obtains an energy cost of 0.6841, a PAR of 1.3639, and a DI value of 0, which is much lower than NSGA-II (1.1180, 1.5564, and 3), MOPSO (1.1612, 2.0854, and 5), and MOSGA (1.0722, 1.6246, and 6). This shows that the proposed method is highly effective and accurate for obtaining the regions of the Pareto optimal front where a compromise solution can be found. Another highlight is that

Table 9
Comparative results of the proposed HEMS for different solar PV sizing

Solar PV peak power (kW)	Energy cost	PAR	DI	Total energy purchased (kW)	Total energy sold (kW)
1	0.6841	1.3639	0	50.8435	7.3238
1.5	0.5953	0.9309	0	49.2834	8.7686
2	0.4226	0.9257	0	44.0903	9.9861
2.5	0.3151	0.7306	0	39.4430	10.1382
3.0	0.1796	0.7089	0	37.6983	13.0848

Table 10
Comparative results between the proposed method with different MOEAs.

Case	Methods	Energy cost	PAR	DI	Computational time (s)
Comprehensive HEMS model	AUGMECON-LO	**0.6841**	**1.3639**	**0**	**14.34**
	NSGA-II	1.1180	1.5564	3	646.77
	MOPSO	1.1612	2.0854	5	829.97
	MOSGA	1.0722	1.6246	6	1207.45
Case 1 – HEMS without V2H	AUGMECON-LO	**0.7549**	**1.3658**	**0**	**13.93**
	NSGA-II	0.8808	1.7539	5	632.17
	MOPSO	0.9729	2.3684	6	822.09
	MOSGA	0.9798	2.6482	4	1145.70
Case 2 – HEMS without BESS	AUGMECON-LO	**0.7873**	**1.4482**	**4**	**14.22**
	NSGA-II	0.9664	1.5705	5	500.31
	MOPSO	1.0578	1.8538	11	781.88
	MOSGA	0.9330	1.8566	6	1047.75
Case 3 – HEMS without storage capacity	AUGMECON-LO	**0.8549**	**1.4619**	**5**	**13.93**
	NSGA-II	1.1080	1.5140	6	516.625
	MOPSO	1.1600	2.3110	8	772.45
	MOSGA	1.1044	1.9593	6	1029.13

AUGMECON-LO obtains the best results and has the lowest computation time for all the cases. As the HEMS optimization under study is currently applied to a single home, it is necessary to determine the optimal solution within the lowest possible computation time. Therefore, AUGMECON-LO has great potential and advantages for obtaining a very effective solution to the multi-objective MILP problem, as shown in this study.

4.1.7. Sensitivity analysis of the proposed AUGMECON-LO

In this section, the effect of AUGMECON-LO on the results is discussed. AUGMECON-LO can control the density of Pareto optimal solutions obtained by precisely adjusting the values of q_2 and q_3. The higher the number of grid points, the denser the number of obtained Pareto optimal sets. However, this also requires more computational time. For a more detailed analysis, we perform a multi-objective MILP problem for a comprehensive HEMS model with different numbers of grid points, as shown in Table 11. When the number of grid points is increased from 5 to 10, the number of Pareto optimal solutions obtained increases, and the computational time also increases. This is because the number of grid points affects the number of subproblems to be solved, as described in Section 3.2. For example, five grid points are selected for each objective function, resulting in $5\times5=25$ subproblems to be solved, and 24 Pareto optimal solutions are obtained. Some subproblems may contain infeasible solution spaces that are discarded.

The default number of grid points is 10, which is given in the GAMS library (https://www.gams.com/latest/gamslib_ml/libhtml/gamslib_epscm.html). Moreover, the number of grid points can be selected arbitrarily. As shown in Table 11, there is no better solution according to the Pareto dominance concept. It can be seen that the total of seven grid points provides an efficient compromise solution for all three objectives. This also provides an appropriate trade-off between the density of the Pareto optimal set and computation time. Another point worth noting is that the same values for all three objectives are obtained when the number of grid points is equal to 7 and 10. Therefore, in this study, the total number of grid points is 7 (i.e., $q_2 = q_3 = 6$) for all simulations.

Table 11
Comparative results of multi-objective HEMS problem for different numbers of grid points.

Number of grid points	Number of obtained Pareto solutions	Compromise solution			Computational time (s)
		Energy cost	PAR	DI	
5	24	0.7834	1.0230	0	9.31
6	35	0.6783	1.6367	0	11.43
7	47	0.6841	1.3639	0	14.34
8	61	0.6969	1.1691	0	17.81
9	78	0.6793	1.5344	0	22.04
10	97	0.6841	1.3639	0	26.73

4.2. Stochastic model

Although the base case considers day-ahead data for weather and the PEV in the deterministic model, in this section, a scenario-based approach to stochastic HEMS is proposed to handle the uncertainties of solar irradiation, ambient temperature, and initial SOE of the PEV. The stochastic model for the HEMS optimization problem is performed in two stages: scenario generation and scenario reduction.

For scenario generation, the probability distribution function (PDF) of each uncertain parameter can be divided into several class intervals associated with the probability. Accordingly, the solar irradiation uncertainty can be modeled using the Beta PDF. A truncated Gaussian PDF can be used to model the ambient temperature uncertainty and the initial SOE distribution of the PEV (Shafie-Khah & Siano, 2018; Tostado-Véliz et al., 2022b). The 1000 Monte Carlo scenarios for each element of solar irradiance, ambient temperature, and initial SOE of the PEV are combined to form a set of 1000 scenarios. The i^{th} scenario is as follows:

$$S_i = \left[v_{1,i}, \ldots, v_{T,i}, \theta_{1,i}, \ldots, \theta_{T,i}, \varepsilon^{PEV}_{initial,i}\right] \tag{64}$$

A sufficiently large number of scenarios are generated according to suitable PDFs that can effectively handle the stochastic nature of forecast parameters. According to the literature, 1000 scenarios are generally considered sufficient (Tostado-Véliz et al., 2022b). However, it is impractical to solve a large number of scenarios. In this regard, 1000 scenarios are reduced to 10 representative scenarios by applying k-medoids technique-based scenario reduction (Pinto et al., 2020). To this end, the set of generated scenarios is grouped into clusters such that the cluster members are as similar as possible. Subsequently, a cluster can be represented by a single member, which is a medoid in this case. The probability (ω) of each representative scenario can be computed as follows:

$$\omega_r = \frac{size(R_r)}{size(S)} \tag{65}$$

where R_r denotes the r^{th} representative scenario, and S denotes the initial set of initially generated scenarios.

After the scenario generation and scenario reduction phases are completed, the proposed AUGMECON-LO is applied to each scenario independently to find a compromise solution for the energy cost, PAR, and DI objectives. The expected values of the energy cost (*EEC*), PAR (*EPAR*), and DI (*EDI*) for all representative scenarios are as follows:

$$EEC = \sum_{r=1}^{N_\Omega} \omega_r \cdot f_{1,r} \tag{66}$$

$$EPAR = \sum_{r=1}^{N_\Omega} \omega_r \cdot f_{2,r} \tag{67}$$

$$EDI = \sum_{r=1}^{N_\Omega} \omega_r \cdot f_{3,r} \tag{68}$$

where $f_{1,r}$, $f_{2,r}$, $f_{3,r}$ denote the optimal values of the energy cost (f_1), PAR (f_2), and DI (f_3), respectively, for the r^{th} representative scenario, which can be defined as in Eqs. (37), (44), and (48), and N_Ω is the total number of representative scenarios.

To generate scenarios from the Beta PDF and truncated Gaussian PDF, the considered data, including the mean and standard deviation for solar irradiance and ambient temperature, are collected in Madrid (Spain) in 2020 (European Commission, 2022). For the initial SOE of the PEV, 1000 scenarios are generated based on a truncated Gaussian PDF with a mean value of 50%, standard deviation of 25%, and maximum and minimum values of 95% and 30%, respectively. All generated scenarios and representative scenarios for the solar irradiation and ambient temperature are shown in Fig. 20. The initial SOE distribution of the PEV is shown in Fig. 21. Other input data for the HEMS model are kept as the comprehensive case of the deterministic model in Section 4.1.

The impact of uncertainties on HEMS scheduling is investigated using the best-case and worst-case scenarios for each uncertainty element. Fig. 22 presents the purchased energy for the scenario with the highest hourly solar irradiance (i.e., Scenario 4) and the scenario with the lowest hourly solar irradiance (i.e., Scenario 8). From the results obtained, the total energy purchased in Scenario 4 is 51.8573 kW, which is 8.21% less than that in Scenario 8 (56.4957 kW). This significant reduction in the purchased energy can be seen in Fig. 22. As the high solar PV output from the high solar radiation provides a considerable amount for the home load, the HEMS can purchase less energy from the grid in Scenario 4. It can be seen that HEMS can adapt the home load pattern to different solar radiation conditions to take full advantage of solar PV generation.

The uncertainty of the ambient temperature is also an important factor during load scheduling, particularly for thermostatically controlled appliances such as HVAC. Fig. 23 presents the scheduling profiles for HVAC for Scenarios 4 and 8, where Scenario 4 is the one with the highest daily temperature and Scenario 8 is the opposite. With the high daily ambient temperature in Scenario 4, the HVAC system operates in the cooling mode throughout the scheduled time of the day. In contrast, the HVAC system in Scenario 8 only operates in the heating mode with relatively low power consumption owing to the low daily ambient temperature. Based on the input data of ambient temperature, the proposed HEMS correctly controls the HVAC system to maintain the indoor temperature within allowable ranges, as shown in Fig. 24.

The initial SOE of the PEV is considered as an uncertainty parameter in this study. Fig. 25 presents the best- and worst-case scenarios

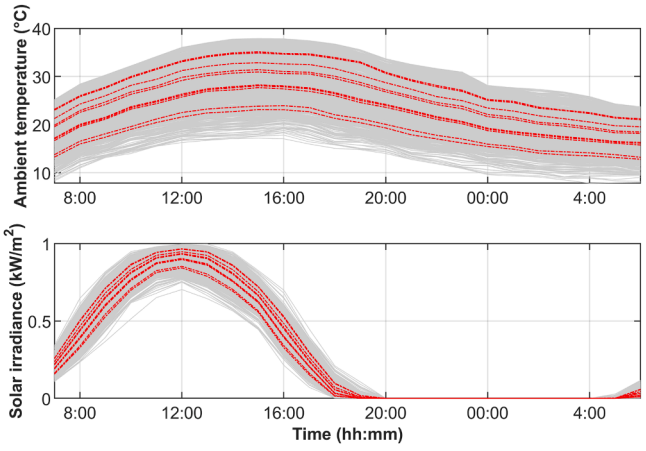

Fig. 20. Generated scenarios (grey line) and representative scenarios (red dotted line) for ambient temperature and solar irradiance.

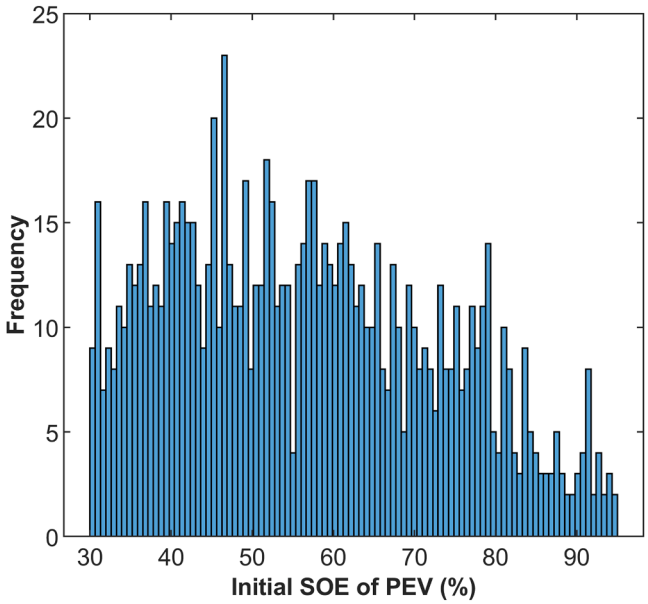

Fig. 21. Initial SOE distribution of the PEV.

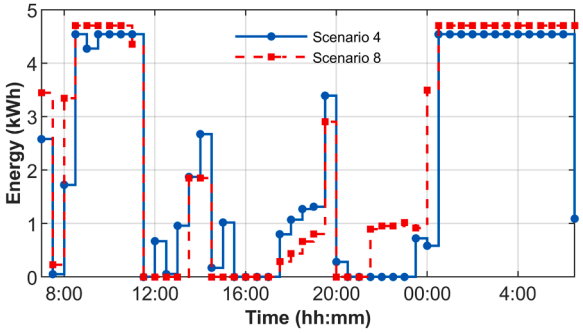

Fig. 22. Energy purchased for Scenarios 4 and 8.

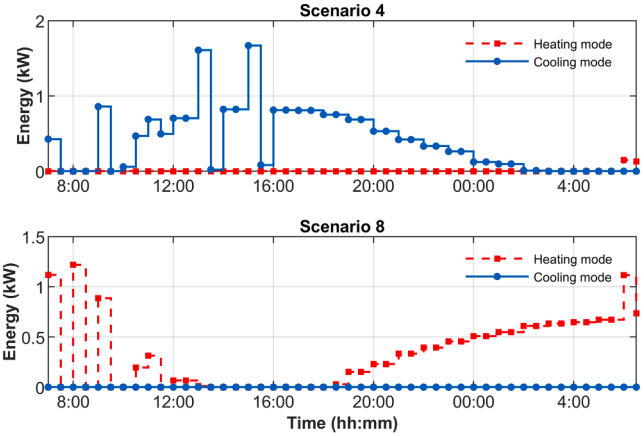

Fig. 23. HVAC power consumption for Scenarios 4 and 8.

associated with the initial SOE of the PEV when it returns home, including a low initial SOE of 40% (Scenario 8) and a high initial SOE of 78% (Scenario 9). In the worst-case scenario, the PEV is forced to spend almost all of its time charging the battery to be fully charged at the time of departure. Evidently, the V2H capability of the PEV is less utilized in the worst-case scenario. In contrast, in the scenario of a PEV departing home with a high initial SOE, the V2H capability is fully exploited to

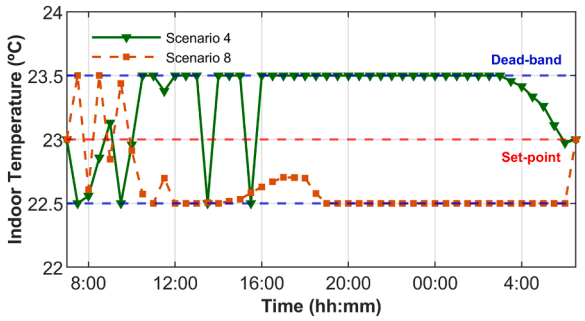

Fig. 24. Indoor temperature for Scenarios 4 and 8.

supply energy to the home load or inject energy back into the utility grid. The total energy of V2H in Scenario 9 is 11.0166 kW, which is significantly higher than that in Scenario 8 (4.4283 kW). Furthermore, the PEV in Scenario 9, with a high initial SOE, also requires less energy to fully charge than in Scenario 8 (16.1991 kW versus 17.9592 kW). The total energy purchased and energy sold in Scenario 9 are 48.6923 and 11.6747 kW, respectively, whereas those in Scenario 8 are 56.4957 and 7.2916 kW, respectively. Accordingly, Scenario 9 has the advantages of purchasing less energy and selling more energy than Scenario 8, as shown in Fig. 26. Despite the uncertainty of the initial SOE of the PEV, the HEMS model successfully provides an optimal charging and discharging plan to effectively utilize the H2V and V2H capabilities while ensuring that the PEV is fully charged at the departure time.

The above analysis shows that uncertainties in weather and PEVs have a significant impact on HEMS scheduling. The expected values of the three objective functions for all scenarios in the stochastic model are listed in Table 12. The expected values from the stochastic model are similar to those obtained from the deterministic model, resulting in expected reductions in energy cost and PAR of 48.17% and 55.64%, respectively. Despite the impact of uncertain factors, the proposed HEMS can provide optimal load patterns to obtain compromise solutions for all scenarios of the stochastic model. It can be concluded that the proposed HEMS model using the AUGMECON-LO method effectively solves the multi-objective HEMS optimization problem for both deterministic and stochastic models.

4.3. Discussion

Optimal coordination of the operation schedule of electrical components and devices at the residential level is very important in smart-grid paradigms. The development of the proposed HEMS can significantly improve the energy cost, home load patterns, and user satisfaction. Based on the literature review, this is the first study to propose a multi-objective MILP paradigm using the AUGMECON-LO method to minimize the energy cost, PAR, and DI objectives via HEMS modeling. Intelligent devices, including solar PV system, BESS, PEV, controllable appliances, and thermostatically controlled appliances, were fully considered in the proposed HEMS model. Furthermore, the advanced technologies of the PEV, namely H2V and V2H, were fully made use of through bidirectional chargers. This study considered energy cost minimization as the most important objective function, whereas PAR and DI objectives were treated as constraints. The multi-objective MILP problem was solved using the AUGMECON-LO method, and a global optimal solution was obtained efficiently.

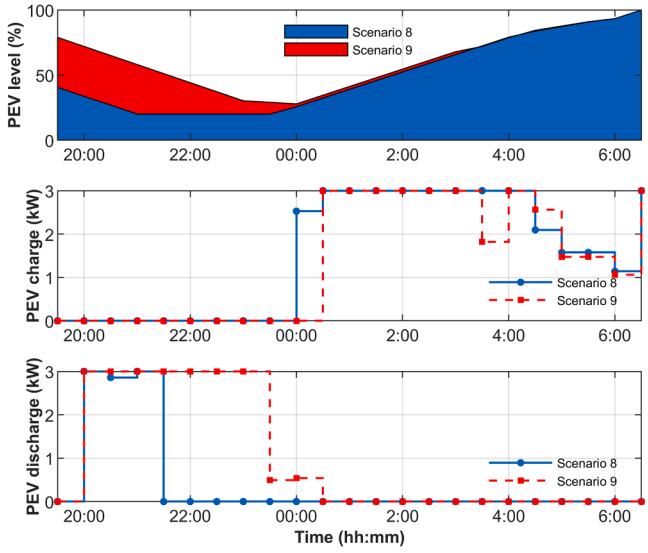

Fig. 25. SOC and SOE of the PEV for Scenarios 8 and 9.

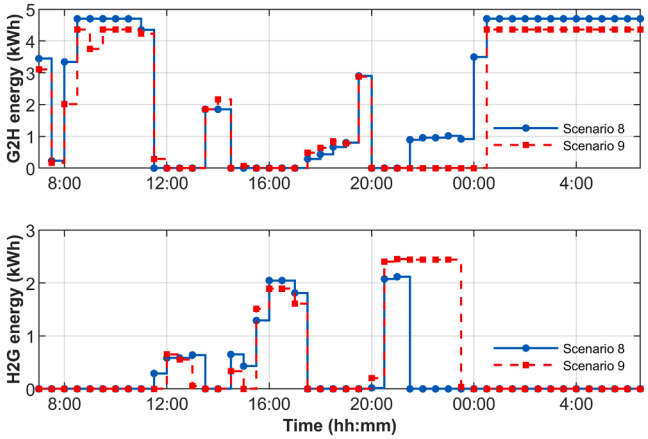

Fig. 26. Energy purchased and sold between HEMS and the utility grid for Scenarios 8 and 9.

Table 12
Results for the stochastic and deterministic models.

Objective	Stochastic model	Deterministic model
Energy cost	0.6813	0.6841
PAR	1.3517	1.3639
DI	0	0

The obtained results show that the proposed multi-objective MILP paradigm based on AUGMECON-LO for HEMS modeling can yield a compromise solution that greatly reduces the energy cost and PAR and maintains the DI value at a minimum. The proposed HEMS model was validated using deterministic and stochastic models. In the deterministic model, single-objective optimization for the HEMS model was first performed to show the conflicting relationship between different objective functions, including cost, PAR, and DI. Indeed, minimizing one objective may lead to undesirable values for other objectives. This demonstrates the necessity of formulating the HEMS problem as a multi-objective problem instead of a single-objective problem. Next, the multi-objective HEMS problem was solved using AUGMECON-LO. The results show that the energy cost and PAR were significantly reduced by 47.96% and 55.24%, respectively, compared to the base-load profile. Simultaneously, the DI value obtained was minimal for the comprehensive HEMS model.

Extensive studies have been conducted to analyze the influence of storage capacity and solar PV sizing on multi-objective HEMS problem. For the analysis of the impact of storage capacity, the simulation results show that HEMS without V2H has an advantage over HEMS without BESS in terms of reducing the energy cost and DI value. The BESS provides a flexible storage solution to store surplus energy from a solar PV system or energy from the grid at intervals of off-peak prices. It also

releases energy during the peak demand or peak price intervals. Hence, the BESS plays a key role in the load scheduling of the smart home investigated herein. The results of this study also reveal that increasing the solar PV system size provides a significant improvement in the reduction of energy cost and PAR. In particular, the energy and PAR costs were reduced by up to 73.75% and 48.02%, respectively, when the solar PV peak power was increased from 1 to 3 kW. Therefore, the installation of a rooftop solar PV system with a high peak power should be considered together with a BESS to capture the full advantage of self-generation in a smart home.

The effectiveness of the proposed AUGMECON-LO was compared with that of NSGA-II, MOPSO, and MOSGA in four case studies. The comparison results obtained from this study indicate that AUGMECON-LO has superior performance compared with NSGA-II, MOPSO, and MOSGA. This is clearly observed in the case of the comprehensive HEMS model, wherein the energy cost, PAR, and DI yielded by AUGMECON-LO (0.6841, 1.3639, and 0) are much better than those yielded by NSGA-II (1.1180, 1.5564, and 3), MOPSO (1.1612, 2.0854, and 5), and MOSGA (1.0722, 1.6246, and 6). Moreover, owing to the uncertainty in weather data and the SOE of the PEV, a multi-objective HEMS problem is proposed in a stochastic model based on a scenario-based approach. Although uncertain parameters such as solar irradiance, ambient temperature, and the SOE of the PEV have a significant influence on the operation of electrical devices, the proposed HEMS still provides an optimal load scheduling profile for all representative scenarios.

Therefore, the proposed model can be considered a promising solution for load scheduling for residential users to bring great economic, technical, and satisfaction benefits. This model can flexibly and efficiently support the participation of residential users in the demand response strategy.

5. Conclusion

In this paper, we proposed a comprehensive HEMS model in a prosumer environment, where solar PV generation, BESS, bidirectional PEV, controllable appliances, and thermostatically controlled appliances in a typical smart home were fully utilized. The proposed HEMS was formulated as a multi-objective MILP problem with three objective functions: energy cost, PAR, and DI objectives. AUGMECON-LO was proposed to address the multi-objective MILP problem in various simulation cases. In the deterministic model, the simulation results of the multi-objective MILP problem reveal that the coordinated operation of all electrical devices can significantly reduce the energy cost and PAR by up to 47.96% and 55.24%, respectively, while keeping DI at the least possible value for a comprehensive HEMS model. Moreover, extensive scenarios were performed for sensitivity analysis to validate the proposed approach. From the analysis of the effects of storage capacity in the three expansion cases, a comprehensive HEMS model has a huge advantage in reducing the energy cost and DI compared to the other studied models. The study also showed that the storage capacity of BESS has a greater impact than the storage capacity of the PEV. Another point worth highlighting is that a greater sizing of the solar PV system could meaningfully mitigate the energy cost and PAR using the proposed HEMS scheduling. In particular, the energy cost and PAR reductions were dramatically reduced by 73.75% and 48.02%, respectively, with an increase in the peak power of the solar PV system from 1 to 3 kW. Moreover, a stochastic model was proposed using a scenario-based approach to handle uncertainty in solar irradiation, ambient temperature, and the SOE of the PEV in multi-objective HEMS optimization problems. The expected values of the three objectives yielded expected reductions in energy cost and PAR of 48.17% and 55.64%, respectively, with minimal DI, which confirms the effectiveness of the proposed approach in providing optimal load scheduling for all representative scenarios, despite the impact of uncertain parameters. Therefore, the proposed multi-objective HEMS paradigm based on AUGMECON-LO successfully defines the optimal scheduling profiles to optimize all three predefined objectives for the different cases under study. In future studies, load scheduling in the proposed HEMS model can be extended to microgrids, where multiple smart homes can exchange energy with each other and with other energy systems, such as wind power plants, solar PV plants, and energy hubs. The proposed AUGMECON-LO method is a promising solution to such problems.

Declaration of Competing Interest

The authors declare that they have no known competing financial interests or personal relationships that could have appeared to influence the work reported in this paper.

Data availability

No data was used for the research described in the article.

Acknowledgments

This work was supported in part by the Korea Institute of Energy Technology Evaluation and Planning (KETEP) and the Ministry of Trade, Industry and Energy (MOTIE) of the Republic of Korea (No. 20204030200060), in part by the National Research Foundation of Korea(NRF) grant funded by the Korea government(MSIT) (NRF-2021R1A4A2001810), and in part by the Soonchunhyang Research Fund.

References

Aghaei, J., Amjady, N., & Shayanfar, H. A. (2011). Multi-objective electricity market clearing considering dynamic security by lexicographic optimization and augmented epsilon constraint method. *Applied Soft Computing, 11*(4), 3846–3858. https://doi.org/10.1016/j.asoc.2011.02.022

Aghaei, J., Shayanfar, H., & Amjady, N. (2009). Multi-objective market clearing of joint energy and reserves auctions ensuring power system security. *Energy Conversion and Management, 50*(4), 899–906. https://doi.org/10.1016/j.enconman.2008.12.027

Alilou, M., Tousi, B., & Shayeghi, H. (2020). Home energy management in a residential smart micro grid under stochastic penetration of solar panels and electric vehicles. *Solar Energy, 212*, 6–18. https://doi.org/10.1016/j.solener.2020.10.063

Alsaidan, I., Khodaei, A., & Gao, W. (2018). A comprehensive battery energy storage optimal sizing model for microgrid applications. *IEEE Transactions on Power Systems, 33*(4), 3968–3980. https://doi.org/10.1109/TPWRS.2017.2769639

Amjady, N., Aghaei, J., & Shayanfar, H. A. (2009). Stochastic multiobjective market clearing of joint energy and reserves auctions ensuring power system security. *IEEE Transactions on Power Systems, 24*(4), 1841–1854. https://doi.org/10.1109/TPWRS.2009.2030364

Anvari-Moghaddam, A., Monsef, H., & Rahimi-Kian, A. (2015). Optimal smart home energy management considering energy saving and a comfortable lifestyle. *IEEE Transactions on Smart Grid, 6*(1), 324–332. https://doi.org/10.1109/TSG.2014.2349352

Arévalo, P., Tostado-Véliz, M., & Jurado, F. (2021). A novel methodology for comprehensive planning of battery storage systems. *Journal of Energy Storage, 37*, Article 102456. https://doi.org/10.1016/j.est.2021.102456

Awais, M., Javaid, N., Aurangzeb, K., Haider, S. I., Khan, Z. A., & Mahmood, D. (2018). Towards effective and efficient energy management of single home and a smart community exploiting heuristic optimization algorithms with critical peak and real-time pricing tariffs in smart grids. *Energies, 11*(11). https://doi.org/10.3390/en11113125. Article 11.

Batchu, R., & Pindoriya, N. M. (2015). Residential demand response algorithms: State-of-the-art, key issues and challenges. In P. Pillai, Y. F. Hu, I. Otung, & G. Giambene (Eds.), *Wireless and satellite systems* (pp. 18–32). Springer International Publishing. https://doi.org/10.1007/978-3-319-25479-1_2.

Chankong, V., & Haimes, Y. Y. (2008). *Multiobjective decision making: Theory and methodology*. Dover (Illustrated edition).

Coello, C. A. C., Pulido, G. T., & Lechuga, M. S. (2004). Handling multiple objectives with particle swarm optimization. *IEEE Transactions on Evolutionary Computation, 8*(3), 256–279. https://doi.org/10.1109/TEVC.2004.826067

Cohon, J. L. (2004). *Multiobjective programming and planning*. Dover Publications (Illustrated edition).

ComEd's Hourly Pricing Program. (n.d.). Retrieved June 7, 2022, from https://hourlypricing.comed.com/.

de Azevedo, R. M., Canha, L. N., Garcia, V. J., Sepúlveda Rangel, C. A., Silva Santana, T. A., & Nadal, Z. I. (2022). Dynamic and proactive matheuristic for AC/DC hybrid smart home energy operation considering load, energy resources and price uncertainties. *International Journal of Electrical Power & Energy Systems, 137*, Article 107463. https://doi.org/10.1016/j.ijepes.2021.107463

Deb, K., Pratap, A., Agarwal, S., & Meyarivan, T. (2002). A fast and elitist multiobjective genetic algorithm: NSGA-II. *IEEE Transactions on Evolutionary Computation, 6*(2), 182–197. https://doi.org/10.1109/4235.996017

Du, P., & Lu, N. (2011). Appliance commitment for household load scheduling. *IEEE Transactions on Smart Grid, 2*(2), 411–419. https://doi.org/10.1109/TSG.2011.2140344

Duman, A. C., Erden, H. S., Gönül, Ö., & Güler, Ö. (2021). A home energy management system with an integrated smart thermostat for demand response in smart grids. *Sustainable Cities and Society, 65*, Article 102639. https://doi.org/10.1016/j.scs.2020.102639

Emami Javanmard, M., Ghaderi, S. F., & Sangari, M. S. (2020). Integrating energy and water optimization in buildings using multi-objective mixed-integer linear programming. *Sustainable Cities and Society, 62*, Article 102409. https://doi.org/10.1016/j.scs.2020.102409

Esmaeel Nezhad, A., Rahimnejad, A., & Gadsden, S. A. (2021). Home energy management system for smart buildings with inverter-based air conditioning system. *International Journal of Electrical Power & Energy Systems, 133*, Article 107230. https://doi.org/10.1016/j.ijepes.2021.107230

Hou, X., Wang, J., Huang, T., Wang, T., & Wang, P. (2019). Smart home energy management optimization method considering energy storage and electric vehicle. *IEEE Access, 7*, 144010–144020. https://doi.org/10.1109/ACCESS.2019.2944878

Huy, T. H. B., Kim, D., & Vo, D. N. (2022). Multiobjective optimal power flow using multiobjective search group algorithm. *IEEE Access, 10*, 77837–77856. https://doi.org/10.1109/ACCESS.2022.3193371

Huy, T. H. B., Nallagownden, P., Truong, K. H., Kannan, R., Vo, D. N., & Ho, N. (2022). Multi-Objective Search Group Algorithm for engineering design problems. *Applied Soft Computing, 126*, Article 109287. https://doi.org/10.1016/j.asoc.2022.109287

Huy, T. H. B., Nguyen, T. P., Mohd Nor, N., Elamvazuthi, I., Ibrahim, T., & Vo, D. N. (2022). Performance improvement of multiobjective optimal power flow-based renewable energy sources using intelligent algorithm. *IEEE Access, 10*, 48379–48404. https://doi.org/10.1109/ACCESS.2022.3170547

Javadi, M. S., Gough, M., Lotfi, M., Esmaeel Nezhad, A., Santos, S. F., & Catalão, J. P. S. (2020). Optimal self-scheduling of home energy management system in the presence of photovoltaic power generation and batteries. *Energy, 210*, Article 118568. https://doi.org/10.1016/j.energy.2020.118568

Javadi, M. S., Nezhad, A. E., Nardelli, P. H. J., Gough, M., Lotfi, M., Santos, S., & Catalão, J. P. S. (2021). Self-scheduling model for home energy management systems considering the end-users discomfort index within price-based demand response programs. *Sustainable Cities and Society, 68*, Article 102792. https://doi.org/10.1016/j.scs.2021.102792

Jin, X., Baker, K., Christensen, D., & Isley, S. (2017). Foresee: A user-centric home energy management system for energy efficiency and demand response. *Applied Energy, 205*, 1583–1595. https://doi.org/10.1016/j.apenergy.2017.08.166

JRC Photovoltaic Geographical Information System (PVGIS)—European Commission. (n. d.). Retrieved June 7, 2022, from https://re.jrc.ec.europa.eu/pvg_tools/en/tools.html.

Khalid, A., Javaid, N., Guizani, M., Alhussein, M., Aurangzeb, K., & Ilahi, M. (2018). Towards dynamic coordination among home appliances using multi-objective energy optimization for demand side management in smart buildings. *IEEE Access, 6*, 19509–19529. https://doi.org/10.1109/ACCESS.2018.2791546

Khaloie, H., Abdollahi, A., Shafie-khah, M., Anvari-Moghaddam, A., Nojavan, S., Siano, P., & Catalão, J. P. S. (2020). Coordinated wind-thermal-energy storage offering strategy in energy and spinning reserve markets using a multi-stage model. *Applied Energy, 259*, Article 114168. https://doi.org/10.1016/j.apenergy.2019.114168

Khaloie, H., Abdollahi, A., Shafie-Khah, M., Siano, P., Nojavan, S., Anvari-Moghaddam, A., & Catalão, J. P. S. (2020). Co-optimized bidding strategy of an integrated wind-thermal-photovoltaic system in deregulated electricity market under uncertainties. *Journal of Cleaner Production, 242*, Article 118434. https://doi.org/10.1016/j.jclepro.2019.118434

Khaloie, H., Anvari-Moghaddam, A., Hatziargyriou, N., & Contreras, J. (2021). Risk-constrained self-scheduling of a hybrid power plant considering interval-based intraday demand response exchange market prices. *Journal of Cleaner Production, 282*, Article 125344. https://doi.org/10.1016/j.jclepro.2020.125344

Khaloie, H., Mollahassani-Pour, M., & Anvari-Moghaddam, A. (2021). Optimal behavior of a hybrid power producer in day-ahead and intraday markets: A bi-objective CVaR-based approach. *IEEE Transactions on Sustainable Energy, 12*(2), 931–943. https://doi.org/10.1109/TSTE.2020.3026066

Khaloie, H., Vallée, F., Lai, C. S., Toubeau, J.-F., & Hatziargyriou, N. D. (2022). Day-ahead and intraday dispatch of an integrated biomass-concentrated solar system: A multi-objective risk-controlling approach. *IEEE Transactions on Power Systems, 37*(1), 701–714. https://doi.org/10.1109/TPWRS.2021.3096815

Kong, X., Sun, B., Kong, D., & Li, B. (2020). Home energy management optimization method considering potential risk cost. *Sustainable Cities and Society, 62*, Article 102378. https://doi.org/10.1016/j.scs.2020.102378

Lin, Y.-H., & Tsai, M.-S. (2015). An advanced home energy management system facilitated by nonintrusive load monitoring with automated multiobjective power scheduling. *IEEE Transactions on Smart Grid, 6*(4), 1839–1851. https://doi.org/10.1109/TSG.2015.2388492

Lokeshgupta, B., & Sivasubramani, S. (2019). Multi-objective home energy management with battery energy storage systems. *Sustainable Cities and Society, 47*, Article 101458. https://doi.org/10.1016/j.scs.2019.101458

Lu, Q., Guo, Q., & Zeng, W. (2022). Optimization scheduling of home appliances in smart home: A model based on a niche technology with sharing mechanism. *International Journal of Electrical Power & Energy Systems, 141*, Article 108126. https://doi.org/10.1016/j.ijepes.2022.108126

Mavrotas, G. (2009). Effective implementation of the ε-constraint method in Multi-Objective Mathematical Programming problems. *Applied Mathematics and Computation, 213*(2), 455–465. https://doi.org/10.1016/j.amc.2009.03.037

Mavrotas, G., & Florios, K. (2013). An improved version of the augmented ε-constraint method (AUGMECON2) for finding the exact pareto set in multi-objective integer programming problems. *Applied Mathematics and Computation, 219*(18), 9652–9669. https://doi.org/10.1016/j.amc.2013.03.002

Nezhad, A. E., Javadi, M. S., & Rahimi, E. (2014). Applying augmented ε-constraint approach and lexicographic optimization to solve multi-objective hydrothermal generation scheduling considering the impacts of pumped-storage units. *International Journal of Electrical Power & Energy Systems, 55*, 195–204. https://doi.org/10.1016/j.ijepes.2013.09.006

Paterakis, N. G., Erdinç, O., Bakirtzis, A. G., & Catalão, J. P. S. (2015). Optimal household appliances scheduling under day-ahead pricing and load-shaping demand response strategies. *IEEE Transactions on Industrial Informatics, 11*(6), 1509–1519. https://doi.org/10.1109/TII.2015.2438534

Pinto, E. S., Serra, L. M., & Lázaro, A. (2020). Evaluation of methods to select representative days for the optimization of polygeneration systems. *Renewable Energy, 151*, 488–502. https://doi.org/10.1016/j.renene.2019.11.048

Rahim, S., Javaid, N., Ahmad, A., Khan, S. A., Khan, Z. A., Alrajeh, N., & Qasim, U. (2016). Exploiting heuristic algorithms to efficiently utilize energy management controllers with renewable energy sources. *Energy and Buildings, 129*, 452–470. https://doi.org/10.1016/j.enbuild.2016.08.008

Rezaee Jordehi, A. (2020). Enhanced leader particle swarm optimisation (ELPSO): A new algorithm for optimal scheduling of home appliances in demand response programs. *Artificial Intelligence Review, 53*(3), 2043–2073. https://doi.org/10.1007/s10462-019-09726-3

Roman, C., & Rosehart, W. (2006). Evenly distributed pareto points in multi-objective optimal power flow. *IEEE Transactions on Power Systems, 21*(2), 1011–1012. https://doi.org/10.1109/TPWRS.2006.873010

Rosin, A., Link, S., Lehtla, M., Martins, J., Drovtar, I., & Roasto, I. (2017). Performance and feasibility analysis of electricity price based control models for thermal storages in households. *Sustainable Cities and Society, 32*, 366–374. https://doi.org/10.1016/j.scs.2017.04.008

Shafie-Khah, M., & Siano, P. (2018). A stochastic home energy management system considering satisfaction cost and response fatigue. *IEEE Transactions on Industrial Informatics, 14*(2), 629–638. https://doi.org/10.1109/TII.2017.2728803

Sharifi, A. H., & Maghouli, P. (2019). Energy management of smart homes equipped with energy storage systems considering the PAR index based on real-time pricing. *Sustainable Cities and Society, 45*, 579–587. https://doi.org/10.1016/j.scs.2018.12.019

Tostado-Véliz, M., Arévalo, P., Kamel, S., Zawbaa, H. M., & Jurado, F. (2022a). Home energy management system considering effective demand response strategies and uncertainties. *Energy Reports, 8*, 5256–5271. https://doi.org/10.1016/j.egyr.2022.04.006

Tostado-Véliz, M., Bayat, M., Ghadimi, A. A., & Jurado, F. (2021). Home energy management in off-grid dwellings: Exploiting flexibility of thermostatically controlled appliances. *Journal of Cleaner Production, 310*, Article 127507. https://doi.org/10.1016/j.jclepro.2021.127507

Tostado-Véliz, M., Gurung, S., & Jurado, F. (2022b). Efficient solution of many-objective Home Energy Management systems. *International Journal of Electrical Power & Energy Systems, 136*, Article 107666. https://doi.org/10.1016/j.ijepes.2021.107666

Tostado-Véliz, M., Icaza-Alvarez, D., & Jurado, F. (2021). A novel methodology for optimal sizing photovoltaic-battery systems in smart homes considering grid outages and demand response. *Renewable Energy, 170*, 884–896. https://doi.org/10.1016/j.renene.2021.02.006

Tostado-Véliz, M., León-Japa, R. S., & Jurado, F. (2021). Optimal electrification of off-grid smart homes considering flexible demand and vehicle-to-home capabilities. *Applied Energy, 298*, Article 117184. https://doi.org/10.1016/j.apenergy.2021.117184

Veras, J. M., Silva, I. R. S., Pinheiro, P. R., Rabêlo, R. A. L., Veloso, A. F. S., Borges, F. A. S., & Rodrigues, J. J. P. C. (2018). A multi-objective demand response optimization model for scheduling loads in a home energy management system. *Sensors, 18*(10). https://doi.org/10.3390/s18103207. Article 10.

Wang, H., Meng, K., Luo, F., Dong, Z. Y., Verbič, G., Xu, Z., & Wong, K. P. (2013). Demand response through smart home energy management using thermal inertia. In *2013 Australasian Universities Power Engineering Conference (AUPEC)* (pp. 1–6). https://doi.org/10.1109/AUPEC.2013.6725442

Wang, P., Zhang, Z., Fu, L., & Ran, N. (2021). Optimal design of home energy management strategy based on refined load model. *Energy, 218*, Article 119516. https://doi.org/10.1016/j.energy.2020.119516

Wang, X., Mao, X., & Khodaei, H. (2021). A multi-objective home energy management system based on internet of things and optimization algorithms. *Journal of Building Engineering, 33*, Article 101603. https://doi.org/10.1016/j.jobe.2020.101603

Yahia, Z., & Pradhan, A. (2020). Multi-objective optimization of household appliance scheduling problem considering consumer preference and peak load reduction. *Sustainable Cities and Society, 55*, Article 102058. https://doi.org/10.1016/j.scs.2020.102058

Yu, B., Sun, F., Chen, C., Fu, G., & Hu, L. (2022). Power demand response in the context of smart home application. *Energy, 240*, Article 122774. https://doi.org/10.1016/j.energy.2021.122774

Zheng, Z., Sun, Z., Pan, J., & Luo, X. (2021). An integrated smart home energy management model based on a pyramid taxonomy for residential houses with photovoltaic-battery systems. *Applied Energy, 298*, Article 117159. https://doi.org/10.1016/j.apenergy.2021.117159

Zupančič, J., Filipič, B., & Gams, M. (2020). Genetic-programming-based multi-objective optimization of strategies for home energy-management systems. *Energy, 203*, Article 117769. https://doi.org/10.1016/j.energy.2020.117769